NASA
Technical
Paper
2401

March 1985

# Wind-Tunnel Investigation at Supersonic Speeds of a Remote-Controlled Canard Missile With a Free-Rolling-Tail Brake Torque System

A. B. Blair, Jr.



Date for general release March 1987



NASA

NASA
Technical
Paper
2401

1985

# Wind-Tunnel Investigation at Supersonic Speeds of a Remote-Controlled Canard Missile With a Free-Rolling-Tail Brake Torque System

A. B. Blair, Jr.

*Langley Research Center*
*Hampton, Virginia*

National Aeronautics
and Space Administration

**Scientific and Technical
Information Branch**

## Summary

An experimental wind-tunnel investigation has been conducted at Mach numbers of 1.70, 2.16, and 2.86 to determine the static aerodynamic characteristics of a cruciform canard-controlled missile with fixed or free-rolling tail-fin afterbodies. Mechanical coupling effects of the free-rolling-tail afterbody were investigated by using an electronic/electromagnetic brake system that provided arbitrary tail-fin brake torques with continuous measurements of tail-to-mainframe torque and tail roll rate. Remote-controlled canards were deflected to provide pitch, yaw, and roll control.

The results of the investigation indicate that the induced rolling-moment coefficients due to canard yaw control are reduced and linearized for the free-rolling-tail (free-tail) configuration. The canards of the free-tail configuration provided conventional roll control for the entire angle-of-attack test range. For the free-tail configuration, the induced rolling-moment coefficient due to canard yaw control increased and the canard roll control decreased with increases in brake torque, which simulated bearing friction torque. It appears that a compromise in regard to bearing friction, for example, low-cost bearings with some friction, may allow satisfactory free-tail aerodynamic characteristics that include reductions in adverse rolling-moment coefficients and lower tail roll rates.


## Introduction

It is well documented that missile configurations utilizing forward control surfaces experience adverse induced rolling moments at supersonic Mach numbers. (See refs. 1 to 3.) For these forward-controlled configurations, the need is either to reduce or eliminate the induced rolling moments or to provide an efficient system for their control.

One approach that was suggested in reference 4 uses the free-rolling-tail concept to reduce adverse rolling moments on a canard-controlled missile. A free-rolling tail reduces the rolling moments by uncoupling the tail from the missile airframe and also allows canard roll control at low angles of attack. The free-rolling-tail concept gives canard-controlled missiles more simplicity and modular flexibility by having a single cruciform canard control system that provides pitch, yaw, and roll control.

The idea of using free-rolling tail fins is not new. From 1950 to 1960, NASA and its predecessor, NACA, investigated a number of roll-control devices in free flight as part of their aerodynamic control research program for missiles and airplanes. For some of these tests, a free-rolling tail-fin assembly was used on the missile airframes, not only to provide the models with longitudinal and directional stability, but also to eliminate unwanted induced rolling moments that were generated by the various roll controls under investigation (refs. 5 and 6). In many cases, the free-rolling tails were on nonmaneuvering missile systems (e.g., boost-glide trajectories at low angles of attack). More recently, the U.S. Navy has conducted research (see refs.7 to 9) using the rolling-tail concept on free-fall stores and missiles.

A preliminary investigation of a canard-controlled missile with fixed and free-rolling tail fins has been reported (ref. 10). The present paper presents the results of a wind-tunnel investigation whose purpose was to extend the fixed and free-tail aerodynamic data base of reference 10 by investigating the mechanical coupling effects of a free-rolling-tail afterbody on a canard-controlled missile with pitch, yaw, and roll control. A summary of the significant findings has been reported in reference 11.

The tests were conducted in the Langley Unitary Plan Wind Tunnel at Mach numbers of 1.70, 2.16, and 2.86. The nominal angle-of-attack range was $-4^\circ$ to $18^\circ$ at a model (canard) roll angle of $0^\circ$ and at a Reynolds number of $6.6 \times 10^6$ per meter ($2.0 \times 10^6$ per foot).

## Symbols

The aerodynamic coefficient data are referred to the body-axis system, which is fixed in the vertical and horizontal planes. The moment reference center is located aft of the model nose at 59.72 percent of the body length.

Values are given in both SI and U.S. Customary Units. The measurements and calculations were made in U.S. Customary Units. Factors relating the two systems are given in reference 12.

| | |
|---|---|
| $A$ | reference area (based on body diameter), 0.003167 $m^2$ (0.034089 $ft^2$) |
| $C_A$ | axial-force coefficient, $\frac{\text{Axial force}}{qA}$ |
| $C_{A,b}$ | base axial-force coefficient, $\frac{\text{Base axial force}}{qA}$ |
| $C_l$ | rolling-moment coefficient, $\frac{\text{Rolling moment}}{qAd}$ |
| $C_m$ | pitching-moment coefficient, $\frac{\text{Pitching moment}}{qAd}$ |
| $C_N$ | normal-force coefficient, $\frac{\text{Normal force}}{qA}$ |
| $C_n$ | yawing-moment coefficient, $\frac{\text{Yawing moment}}{qAd}$ |
| $C_Y$ | side-force coefficient, $\frac{\text{Side force}}{qA}$ |
| $d$ | reference body diameter, 6.350 cm (2.500 in.) |
| $M$ | free-stream Mach number |
| $q$ | free-stream dynamic pressure |
| $\alpha$ | angle of attack, deg |

$\delta_i$ angular control deflection of canard panel where subscript $i$ denotes panel 1, 2, 3, or 4 shown in sketch A, deg

$\delta_{pitch}$ pitch-control deflection of canards 2 and 4 (sketch A), positive leading edge up, $(\delta_2 + \delta_4)/2$, deg

$\delta_{roll}$ roll-control deflection (aileron); deflection of canards 2 and 4 (sketch A), individual canards are each deflected indicated amount; positive to provide clockwise model rotation when viewed from rear, deg

$\delta_{yaw}$ yaw-control deflection of canards 1 and 3 (sketch A), positive for leading edge right when viewed from rear, $(\delta_1 + \delta_3)/2$, deg

$\phi$ model roll angle; positive for clockwise roll when viewed from rear (for $\phi = 0°$, canards are in vertical and horizontal planes), deg

$\dot{\phi}_{tail}$ roll rate of tail-fin afterbody; positive for clockwise roll when viewed from rear, rpm

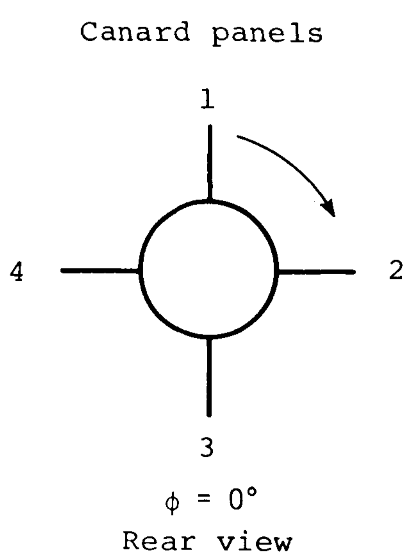


Sketch A

## Apparatus and Tests

### Wind Tunnel

Tests were conducted in the low-Mach-number test section of the Langley Unitary Plan Wind Tunnel, which is a variable-pressure, continuous-flow facility. The test section is approximately 2.13 m (7.0 ft) long and 1.22 m (4.0 ft) square. The nozzle leading to the test section is of the asymmetric sliding-block type, which permits a continuous variation in Mach number from about 1.5 to 2.9. (See ref. 13.)

### Model Concept

To evaluate the mechanical coupling effects of a free-rolling-tail afterbody on a canard-controlled missile, a modified general research missile model was used. Details of the model are shown in figure 1, and photographs of the model are shown in figure 2. The model was a cruciform missile configuration that consisted of a remote-controlled canard forebody with a pointed tangent ogive nose and a cylindrical body that incorporated an electronic/electromagnetic braking system. This braking system was interfaced with a tail-fin afterbody that was either fixed or free rolling. The canards and tail fins had slab cross sections with beveled leading and trailing edges. For both the fixed-tail and free-rolling-tail configurations, the remote-controlled canards were deflected to provide pitch, yaw, and roll control.

The remote-controlled canards were the primary method for inducing tail-fin rotation, since the tail fins were not deflected. Remotely controlled canards provided a selective and responsive control of the canard-generated flow fields produced by the various deflections for pitch, yaw, and roll control. Many of these canard flow fields produce tail flow environments that will spin a free-to-roll tail afterbody.

The electronic/electromagnetic brake system provides arbitrary tail-fin brake torques with continuous measurements of tail-to-mainframe torque and tail roll rate. The brake system assembly is shown in figure 1(c). The free-tail afterbody is mounted on a set of low-friction ball bearings and is coupled to an electromagnet by a free-floating torque brake disc, which makes up part of the magnetic path. The brake disc is held to the electromagnet with a force proportional to a command current. The friction between the brake disc and the electromagnet produces the desired torque. Each sliding surface has a nonmagnetic hard surface coating to reduce wear and produce a magnetic gap to remove residual magnetism when the current goes to zero. The electromagnet is mounted to a one-component strain-gauge torque balance that measures tail brake reaction torques while the tail is rotating in either direction. The electromagnet can provide command brake torque (absolute values) from 0 to 0.68 N-m (0 to 6.0 in-lbf) and is capable of holding selected values for various tail flow conditions by using feedback control from the brake torque balance in combination with electronic servo amplifier circuits. For fixed-tail configurations, the tail-fin afterbody can be aligned ("inline" or "+" position) or interdigitated ("x" position) with respect to the canards by using a lock screw.

Tail-fin roll rates are measured by a transducer composed of an infrared emitter and phototransistor mounted in the coil slot of the electromagnet. A coded reflecting ring is mounted on the brake disc to reflect pulses of light from the infrared emitter to the phototransistor, which converts them to electrical pulses to obtain the tail-fin roll rate. As a safety precaution, the roll rates were limited to ±1000 rpm with an accuracy of ±25 rpm.

By using the electronic/electromagnetic braking system, several simulated bearing friction torques (mechanical coupling effects) can be evaluated with respect to their effects on missile aerodynamics, and results can be presented along with the fixed and free-tail (no brake friction) data. Perhaps there is a compromise in regard to bearing friction, for example, low-cost bearings with some friction, that will allow satisfactory aerodynamic stability and control characteristics while reducing adverse induced roll effects and maintaining low tail-fin roll rates.

## Test Conditions

Tests were performed at the following tunnel conditions:

| Mach number | Stagnation temperature | | Stagnation pressure (absolute) | | Reynolds number | |
|---|---|---|---|---|---|---|
| | K | °F | kPa | lbf/ft$^2$ | per meter | per foot |
| 1.70 | 325 | 125 | 53.3 | 1113 | $6.6 \times 10^6$ | $2.0 \times 10^6$ |
| 2.16 | 325 | 125 | 64.6 | 1349 | $6.6 \times 10^6$ | $2.0 \times 10^6$ |
| 2.86 | 325 | 125 | 92.6 | 1934 | $6.6 \times 10^6$ | $2.0 \times 10^6$ |

The dew point temperature measured at stagnation pressure was maintained below 239 K (−30°F) to assure negligible condensation effects. All tests were performed with boundary-layer transition strips 1.02 cm (0.40 in.) aft of the leading edges. The strips were measured streamwise on both sides of the canards and tail fins and located 3.05 cm (1.20 in.) aft of the body nose. The transition strips were approximately 0.157 cm (0.062 in.) wide and were composed of No. 50 sand grains sprinkled in acrylic plastic (ref. 14).

## Measurements

Aerodynamic forces and moments on the model were measured by means of a six-component electrical strain-gauge balance housed within the model. The balance was attached to a sting which was, in turn, rigidly fastened to the model support system. Balance chamber pressure (base pressure) was measured by means of a single static-pressure orifice located in the vicinity of the balance.

The canards were deflected remotely by four small motors, and deflection angles were measured (accuracy of ±0.1°) by four potentiometers within the model forebody. Continuous measurements of command tail-to-mainframe torque and tail roll rate (rpm) were obtained by the electronic/electromagnetic brake system. A one-component strain-gauge torque balance capable of measuring torque values of ±0.68 N-m (±6.0) in-lbf was mounted to the electromagnet. This balance measured tail brake reaction torques while the tail was rotating in either direction. Tail-fin roll rates are measured by a transducer composed of an infrared emitter and phototransistor mounted in the coil slot of the electromagnet. A coded ring mounted on the rotating brake disc reflected the pulses of light from the infrared emitter to obtain tail-fin roll rates. As a safety precaution, the roll rates were limited to ±1000 rpm with an accuracy of ±25 rpm.

## Corrections

The model angles of attack have been corrected for deflection of the balance and sting due to aerodynamic loads. In addition, angles of attack have been corrected for tunnel flow misalignment. The axial-force-coefficient data have been adjusted to free-stream static pressure acting over the model base. Typical measured values of base axial-force coefficient are presented in figure 3.

# Presentation of Results

The results of this investigation are shown in the following figures:

## Discussion

The effect of fixed and free-rolling tail fins on the longitudinal aerodynamic characteristics of the model with zero canard control deflection is presented in figure 4. To make a more meaningful comparison with the free-tail configurations, the fixed-tail data are presented with the tail fins in both the inline ("+") position and interdigitated ("x") position with respect to the canards at $\phi = 0°$. The remote-controlled canards allowed canard settings such that a uniform flow field could be created with no significant asymmetric flow conditions at the tail. Under these conditions, the free-rolling tail fins have a preferred orientation verified from visual observation with only small oscillation angles usually interdigitated with the canards for $\phi = 0°$. For example, this type of tail flow field is verified by the data (zero tail-fin roll rate) shown in figure 4. The pitch characteristics of the free-tail configuration, in general, exhibit the same trends as the fixed-interdigitated-tail configuration. These trends are characterized by pitch-up that coincides with loss of normal-force coefficient. Both the fixed-tail and free-rolling-tail configurations have about the same normal-force curve slope at low angles of attack.

Pitch-control characteristics for the fixed-tail and free-tail configurations are presented in figure 5 for $\delta_{\text{pitch}} = 5°$. The canard pitch control generates a strong symmetrical downwash flow field (e.g., as indicated by the zero tail-fin roll rate). For the fixed-inline-tail configuration, this downwash contributed to pitch-up near $\alpha = 0°$. The fixed-interdigitated-tail and free-tail configurations have similar pitch characteristics for the entire angle-of-attack test range.

The longitudinal and lateral-directional aerodynamic characteristics of the fixed-tail and free-tail configurations with a canard yaw-control setting ($\delta_{\text{yaw}} = -5°$) are presented in figures 6 and 7, respectively. This setting generated a tail flow-field environment that produces changes in tail-fin roll-rate magnitude and spin direction at low to moderate angles of attack. In general, the pitching-moment data for the free-tail configuration are more linear than, and fall between those of, the fixed-tail configurations (fig. 6). For the fixed-tail configuration in figure 7, the data show the usual induced rolling-moment coefficients that are typical for a canard yaw control. These coefficients are reduced and linearized for the free-tail configuration. In general, the level of yaw control of the free-tail configuration is between those of the fixed-tail configurations at low to moderate angles of attack.

The effect of command brake torque values on the lateral-directional aerodynamic characteristics of the free-tail configuration with a canard yaw control ($\delta_{\text{yaw}} = -5°$) is presented in figure 8. These brake torque values simulated absolute increments of bearing friction torque. In this figure, the data show that increases in simulated bearing friction raise the level of induced rolling-moment coefficient in a linear manner toward fixed-tail values, while yaw control remains about the same (at $\alpha \approx 6°$). As expected, there are reductions in tail-fin roll rates with increases in both simulated bearing friction and Mach number. At the highest test Mach number, the tail-fin rotation is stopped by the lowest brake torque command. It appears that a compromise in regard to bearing friction, for example, low-cost bearings with some friction, may allow satisfactory yaw-control characteristics with low tail roll rates while reducing adverse rolling moments.

The longitudinal and lateral-directional aerodynamic characteristics of the fixed-tail and free-tail configurations with a canard roll control ($\delta_{\text{roll}} = 5°$) are presented in figures 9 and 10, respectively. The canard roll control produces a strong asymmetrical flow field at the tail fins, which is demonstrated by the steady-state roll rates of the tail fins at low to moderate angles of attack. For these tail flow conditions, the pitch trends (fig. 9) of the free-tail configuration are similar to those of the fixed-interdigitated-tail configuration except at intermediate angles of attack, where the data are between fixed-tail configurations. In figure 10, the data of the fixed-tail configurations illustrate typical canard roll-control reversals at low angles of attack. The canards of the free-rolling-tail configuration provide conventional roll control for the entire angle-of-attack range. The roll control and tail-fin roll rate are reduced with increases in the absolute value of brake torque, as shown in figure 11.

## Conclusions

An experimental wind-tunnel investigation has been conducted at Mach numbers of 1.70, 2.16, and 2.86 to determine the static aerodynamic characteristics of a cruciform canard-controlled missile with fixed or free-rolling tail-fin afterbodies. Mechanical coupling effects of the free-rolling-tail afterbody were investigated by using an electronic/electromagnetic brake system that provided arbitrary tail-fin brake torques with continuous measurements of tail-to-mainframe torque and tail roll rate. Remote-controlled canards were deflected to provide pitch, yaw, and roll control. The results of the investigation are as follows:

1. In general, for zero tail-fin roll rates, the pitch curves of the free-rolling-tail (free-tail) and fixed-interdigitated-tail configurations exhibit similar characteristics, whereas for nonzero tail-fin roll rates, the free-tail pitch curve falls between those of the fixed-inline-tail and fixed-interdigitated-tail configurations at moderate angles of attack.

2. The induced rolling-moment coefficients due to canard yaw control are reduced and linearized for the free-tail configuration.

3. The canards of the free-tail configuration provided conventional roll control for the entire angle-of-attack test range.

4. For the free-tail configuration, the induced rolling-moment coefficient due to canard yaw control increased and the canard roll control decreased with increases in brake torque, which simulated bearing friction torque.

5. It appears that a compromise in regard to bearing friction, for example, low-cost bearings with some friction, may allow satisfactory free-tail aerodynamic characteristics that include reductions in adverse rolling-moment coefficients and lower tail roll rates.

Langley Research Center
National Aeronautics and Space Administration
Hampton, VA 23665
November 16, 1984

## References

1. Blair, A. B., Jr.: *Aerodynamic Characteristics of a Tandem-Canard Missile at Mach Numbers From 1.83 to 4.63.* NASA TM X-3040, 1974.
2. Burt, James R., Jr.: *The Effectiveness of Canards for Roll Control.* Tech. Rep. RD-77-8, U.S. Army, Nov. 1976. (Available from DTIC as AD A037 077.)
3. Blair, A. B., Jr.; Allen, Jerry M.; and Hernandez, Gloria: *Effect of Tail-Fin Span on Stability and Control Characteristics of a Canard-Controlled Missile at Supersonic Mach Numbers.* NASA TP-2157, 1983.
4. Sawyer, Wallace C.; Jackson, Charlie M., Jr.; and Blair, A. B., Jr.: Aerodynamic Technologies for the Next Generation of Missiles. Paper presented at the AIAA/ADPA Tactical Missile Conference (Gaithersburg, Maryland), Apr. 27–28, 1977.
5. Schult, Eugene D.: *Free-Flight Measurements of the Rolling Effectiveness and Operating Characteristics of a Bellows-Actuated Split-Flap Aileron on a 60° Delta Wing at Mach Numbers Between 0.8 and 1.8.* NACA RM L54H17, 1954.
6. English, Roland D.: *Rocket-Powered-Model Investigation of the Effects of Aeroelasticity on the Rolling Effectiveness of an 8.06-Percent-Scale McDonnell F3H-1 Airplane Wing at Mach Numbers From 0.5 to 1.4—TED No. NACA DE 351.* NACA RM SL54D12, Bur. Aeronaut., 1954.
7. Regan, Frank J.; and Falusi, Mary E.: *The Static and Magnus Aerodynamic Characteristics of the M823 Research Store Equipped With Fixed and Freely Spinning Stabilizers.* NOLTR 72-291, U.S. Navy, Dec. 1, 1972. (Available from DTIC as AD 757 658.)
8. Regan, F. J.; Shannon, J. H. W.; and Tanner, F. J.: *The Joint N.O.L./R.A.E./W.R.E. Research Programme on Bomb Dynamics. Part III. A Low-Drag Bomb With Freely Spinning Stabilizers.* WRE-Report-904 (WR&D), Australian Def. Sci. Serv., June 1973.
9. Darling, John A.: *Elimination of the Induced Roll of a Canard Control Configuration by Use of a Freely Spinning Tail.* NOLTR 72-197, U.S. Navy, Aug. 16, 1972.
10. Blair, A. B., Jr.: *Wind-Tunnel Investigation at Supersonic Speeds of a Canard-Controlled Missile With Fixed and Free-Rolling Tail Fins.* NASA TP-1316, 1978.
11. Blair, A. B., Jr.: Remote Control Canard Missile With a Free-Rolling Tail Brake Torque System. *J. Spacecr. & Rockets,* vol. 18, no. 6, Nov.–Dec. 1981, pp. 550–555.
12. *Standard for Metric Practice.* E 380-79, American Soc. Testing & Mater., c.1980.
13. Jackson, Charlie M., Jr.; Corlett, William A.; and Monta, William J.: *Description and Calibration of the Langley Unitary Plan Wind Tunnel.* NASA TP-1905, 1981.
14. Stallings, Robert L., Jr.; and Lamb, Milton: *Effects of Roughness Size on the Position of Boundary-Layer Transition and on the Aerodynamic Characteristics of a 55° Swept Delta Wing at Supersonic Speeds.* NASA TP-1027, 1977.

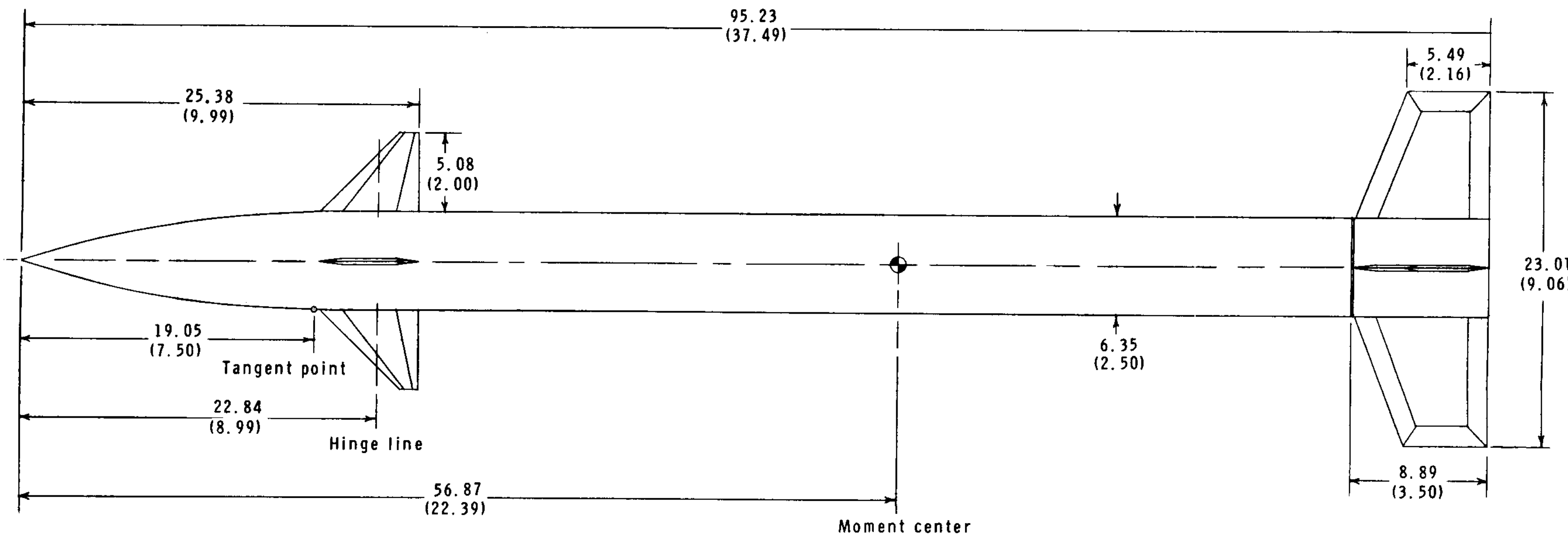


(a) Complete model.

Figure 1. Model details. All dimensions are given in centimeters (inches) unless otherwise indicated.

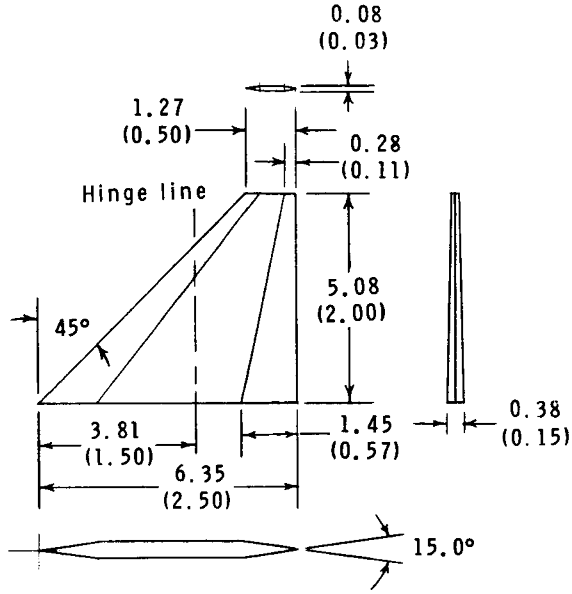


Canard

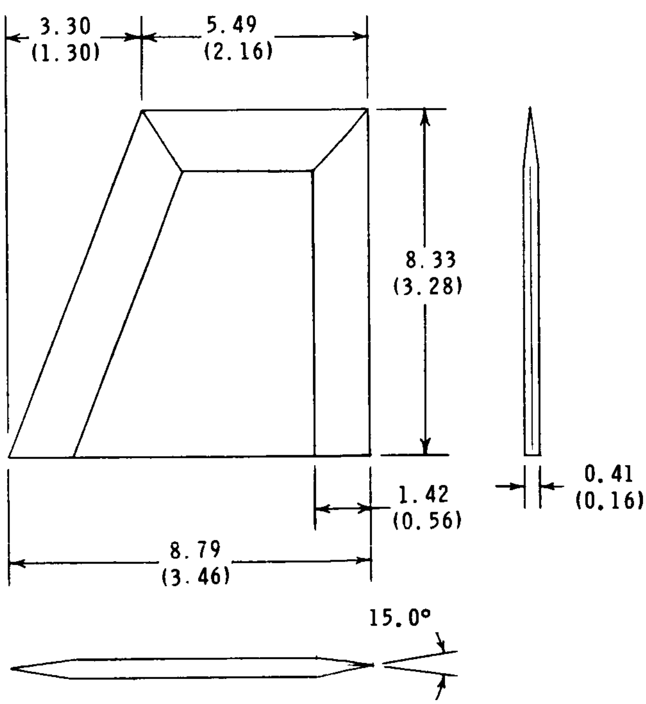


Tail fins

(b) Canard and tail fins.

Figure 1. Continued.

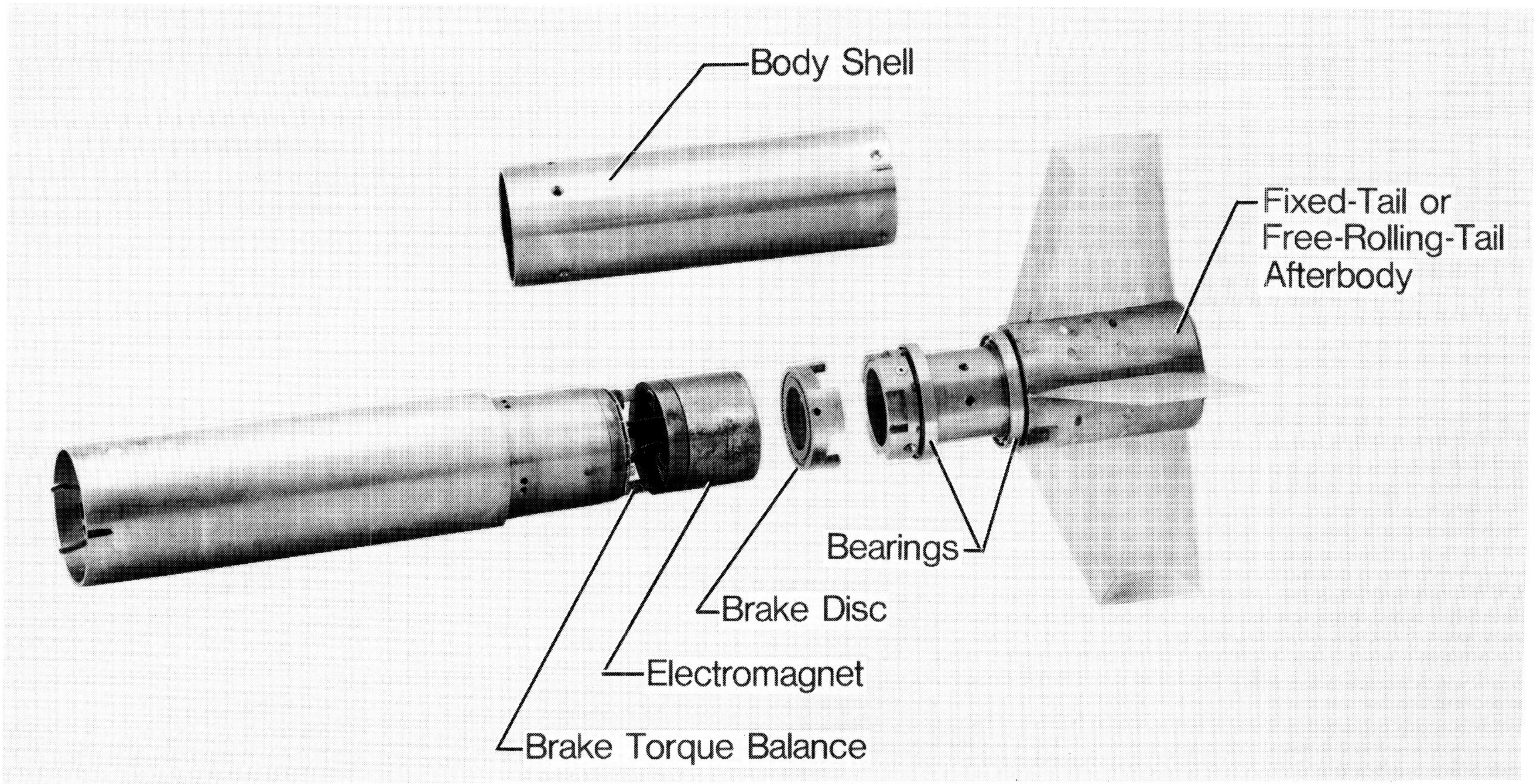


L-84-12,911

(c) Brake system assembly.

Figure 1. Concluded.

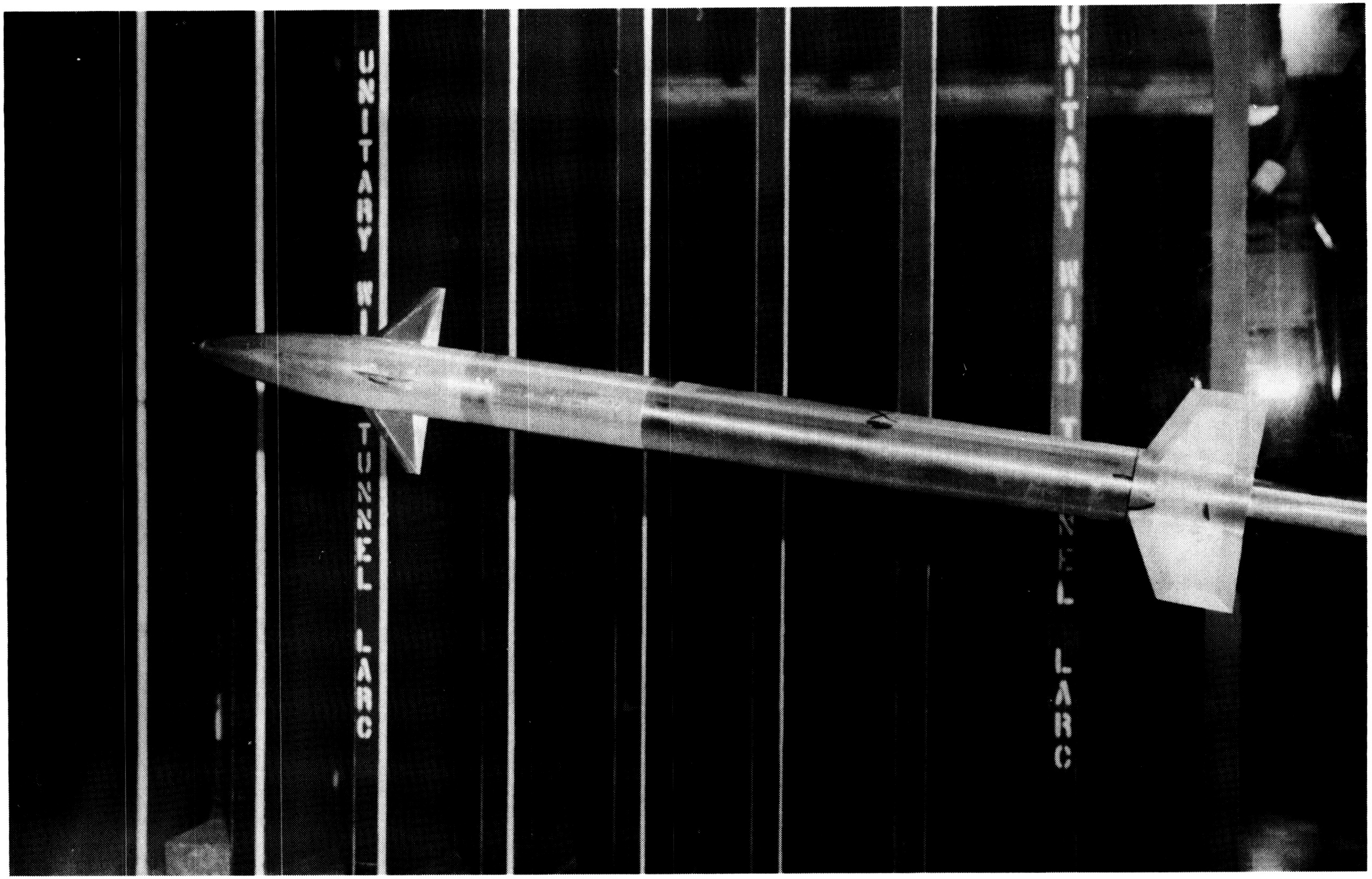


L-80-2785

(a) Fixed tail.

Figure 2. Photographs of model.

L-80-2783

(b) Free tail.

Figure 2. Concluded.

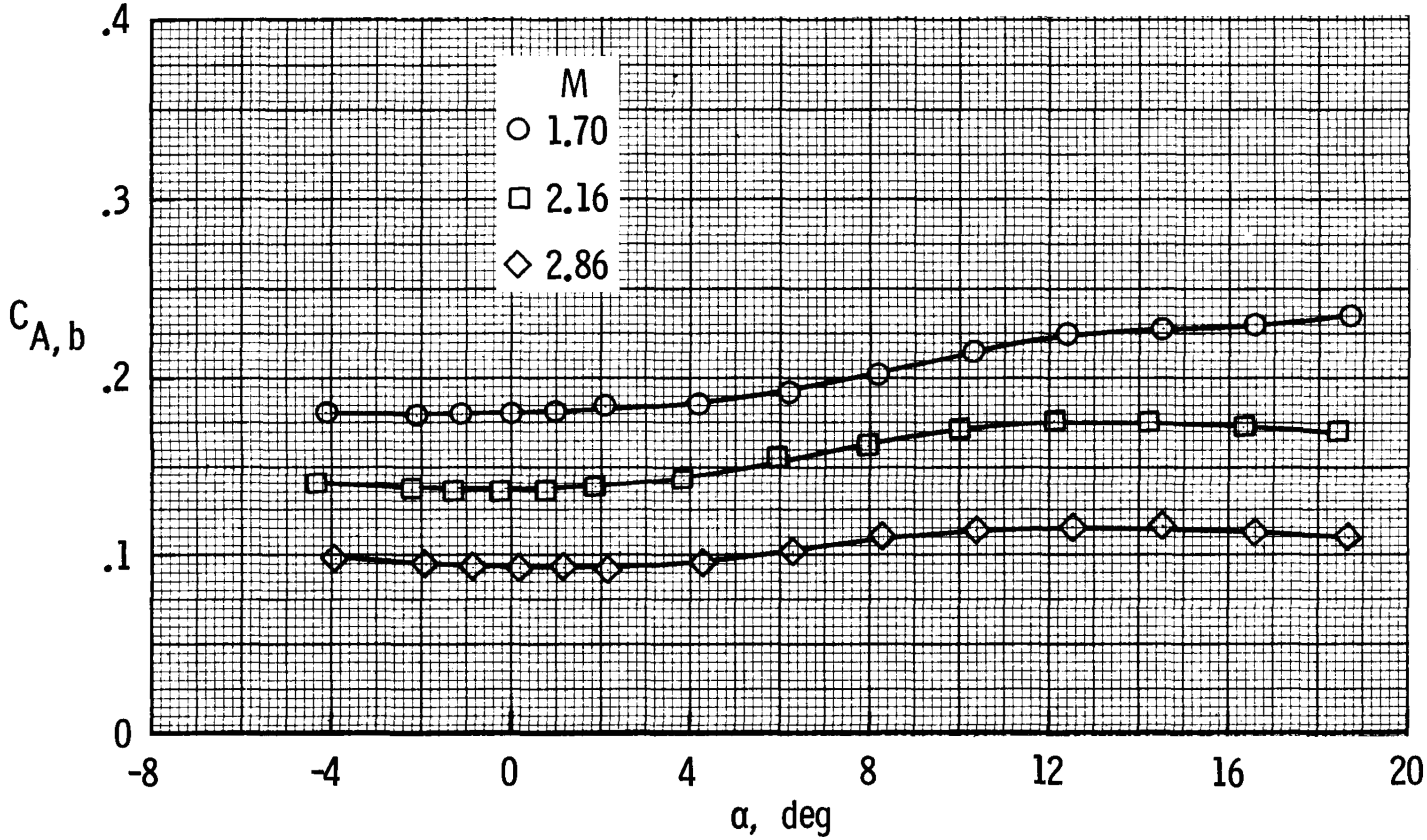


Figure 3. Typical variation of measured base axial-force coefficient with angle of attack. Fixed-tail configuration with zero control deflection.

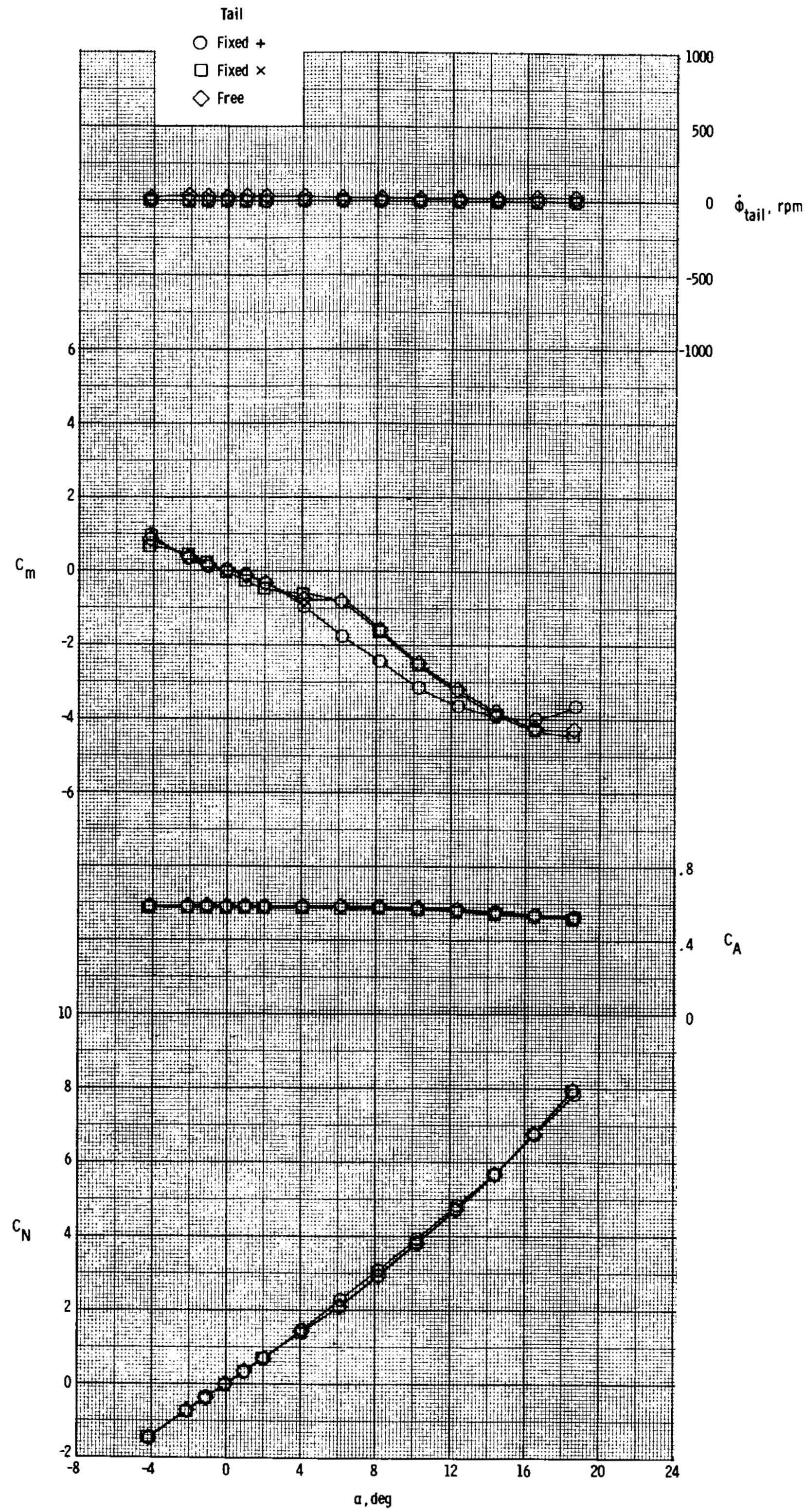


(a) $M = 1.70$.

Figure 4. Effect of fixed and free-rolling tail on longitudinal aerodynamic characteristics of model with zero canard deflection.

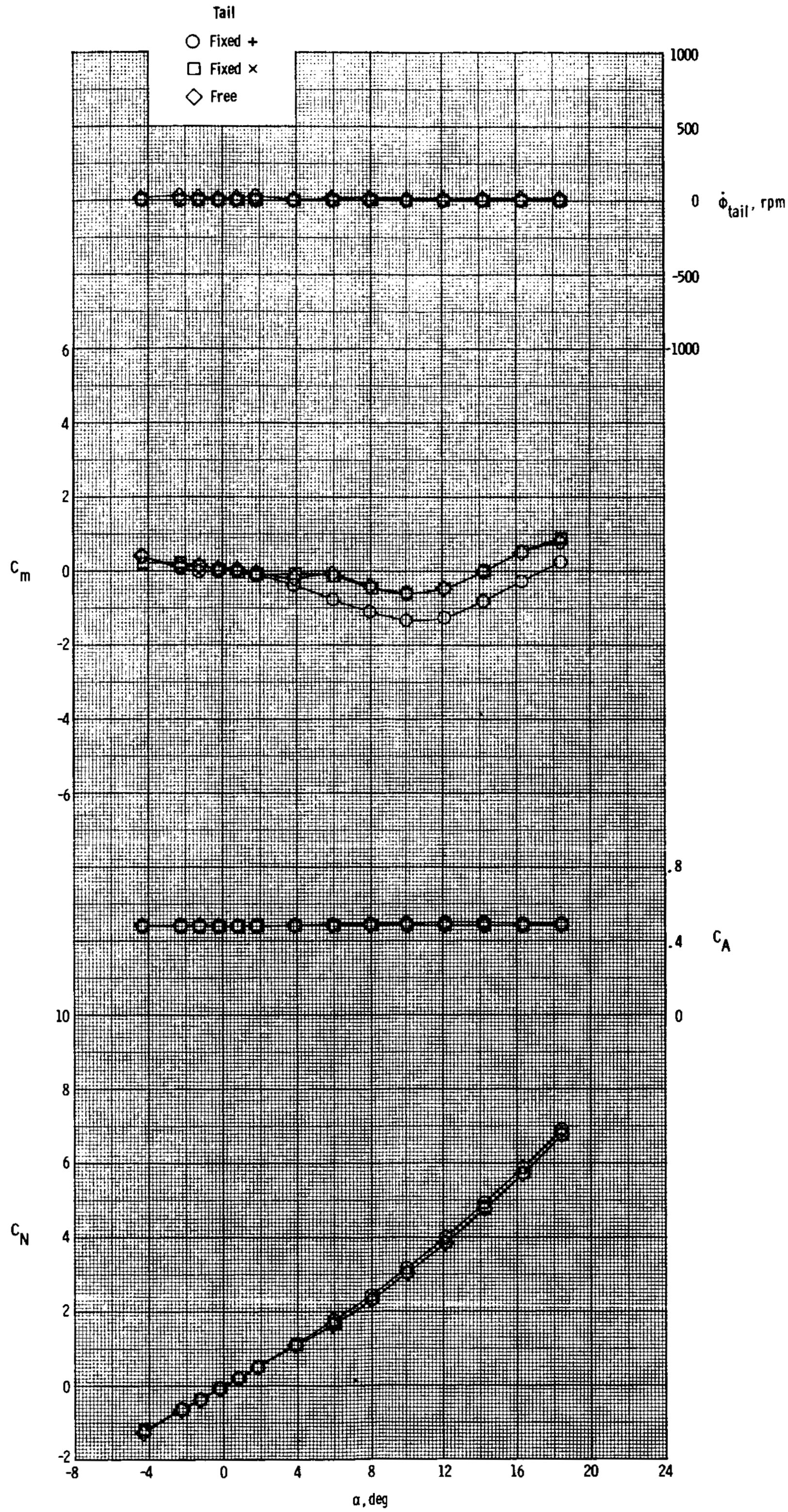


(b) $M = 2.16$.

Figure 4. Continued.

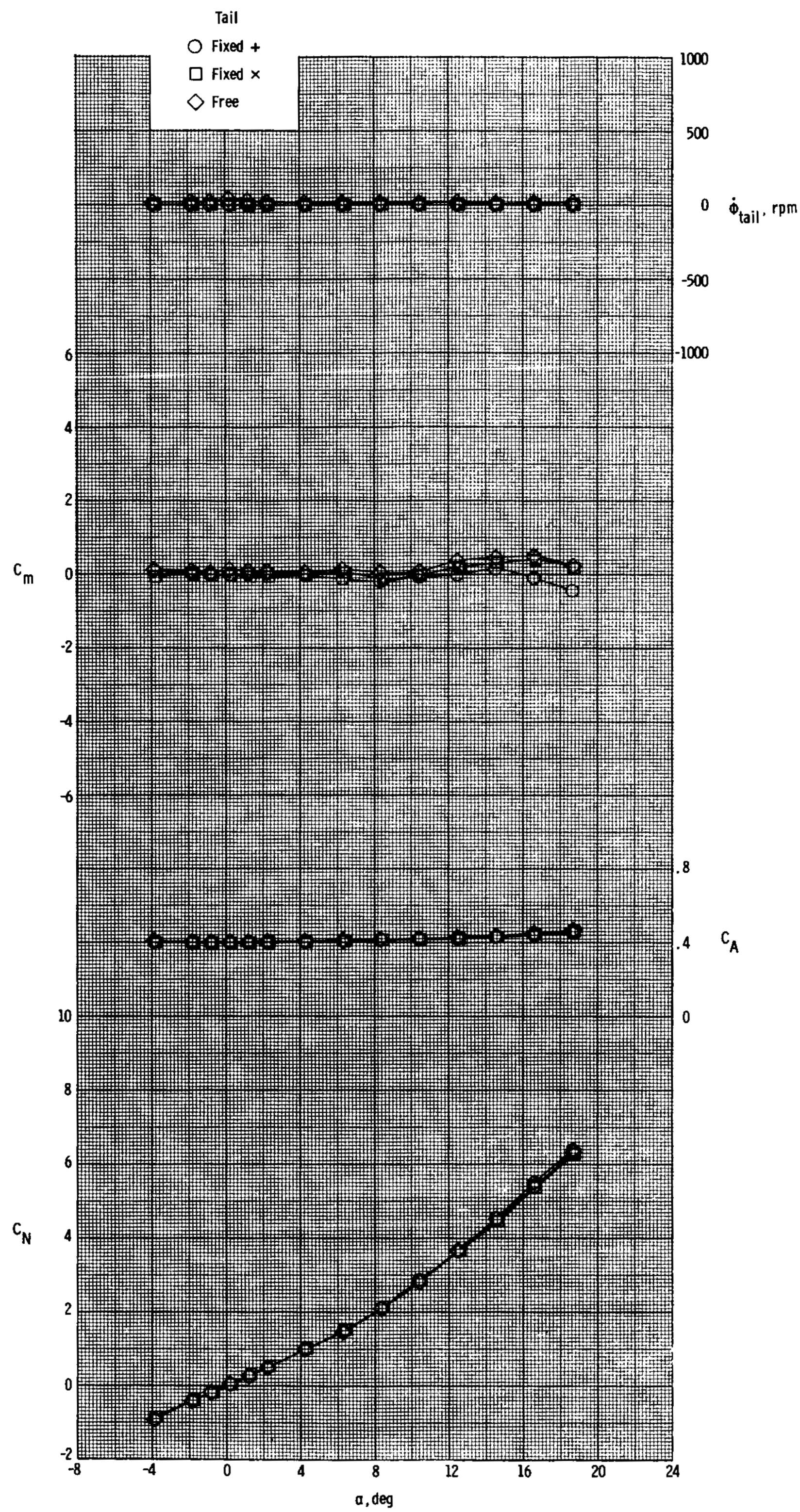


(c) $M = 2.86$.

Figure 4. Concluded.

ORIGINAL PAGE IS
OF POOR QUALITY

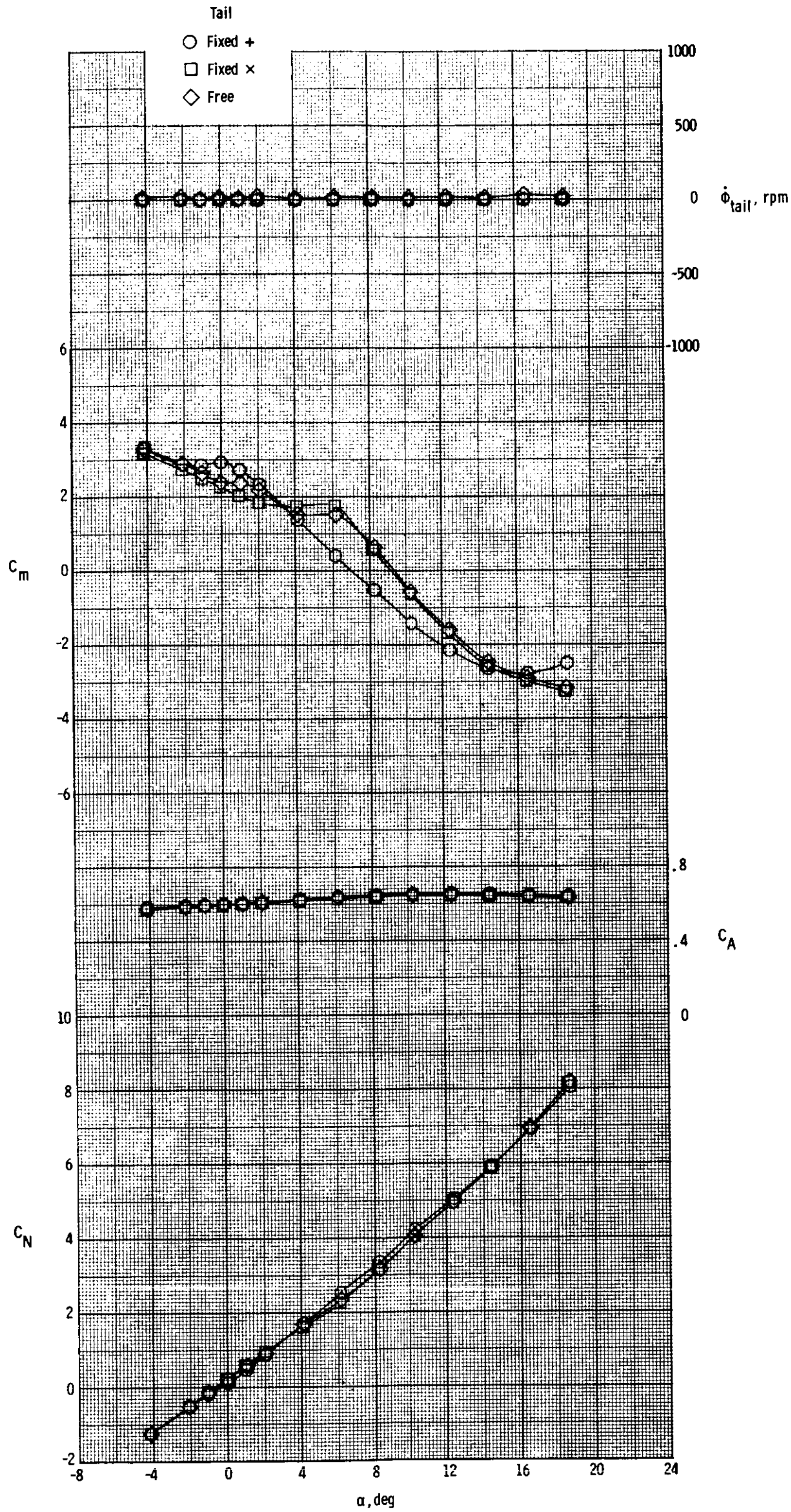


(a) $M = 1.70$.

Figure 5. Effect of fixed and free-rolling tail on pitch-control characteristics of model. $\delta_{pitch} = 5°$.

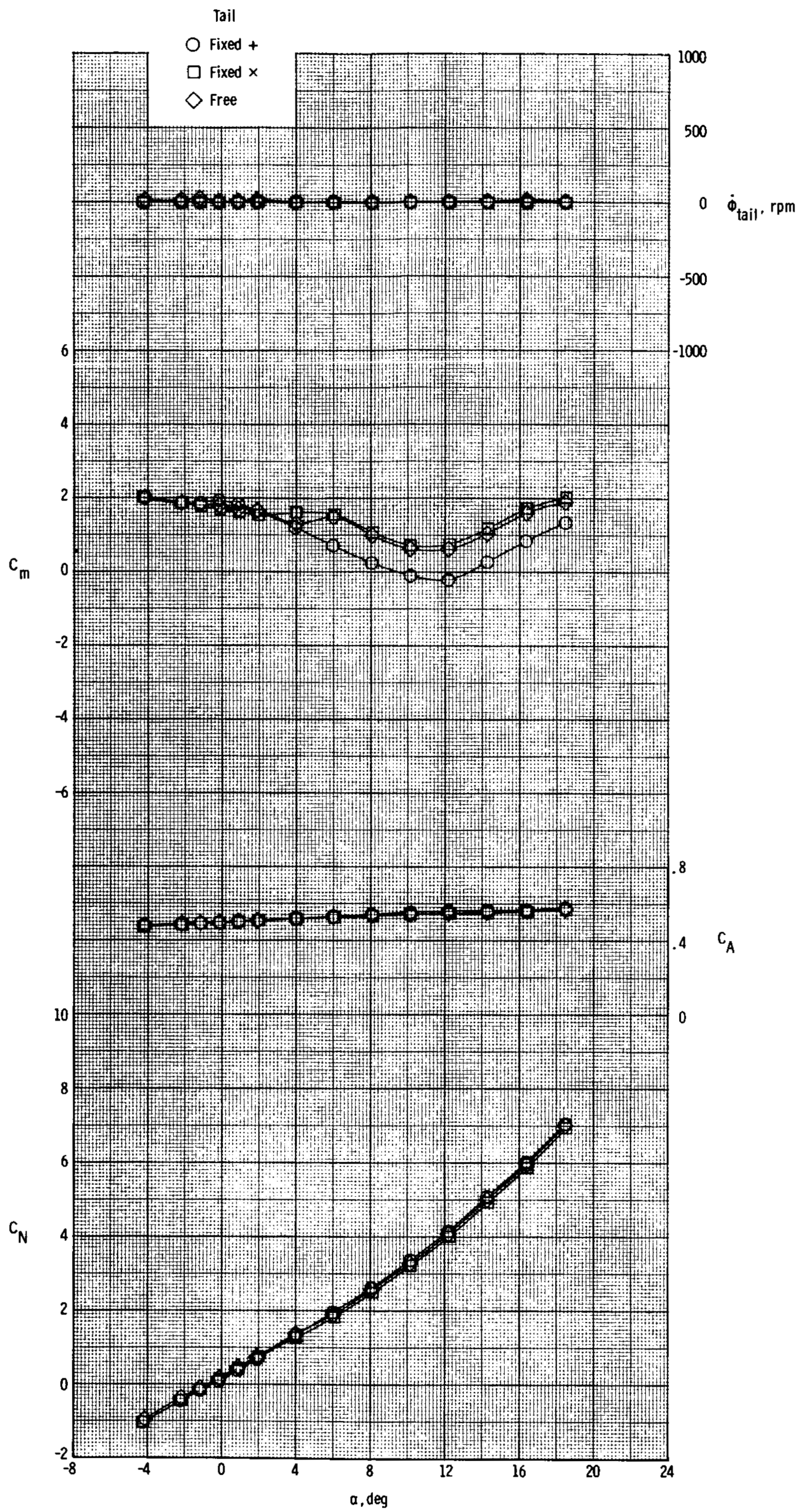


(b) $M = 2.16$.

Figure 5. Continued.

ORIGINAL PAGE IS
OF POOR QUALITY

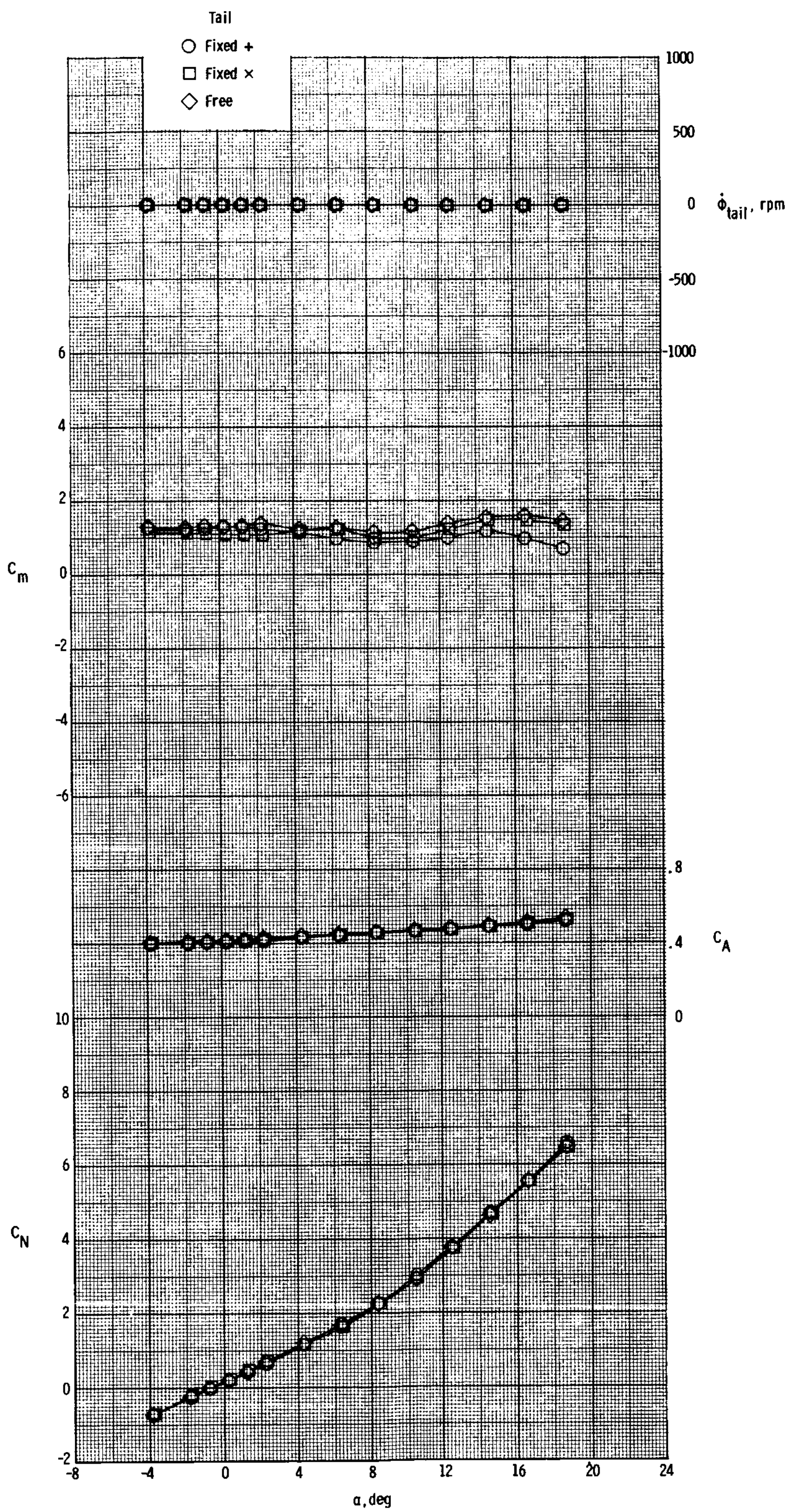


(c) $M = 2.86$.

Figure 5. Concluded.

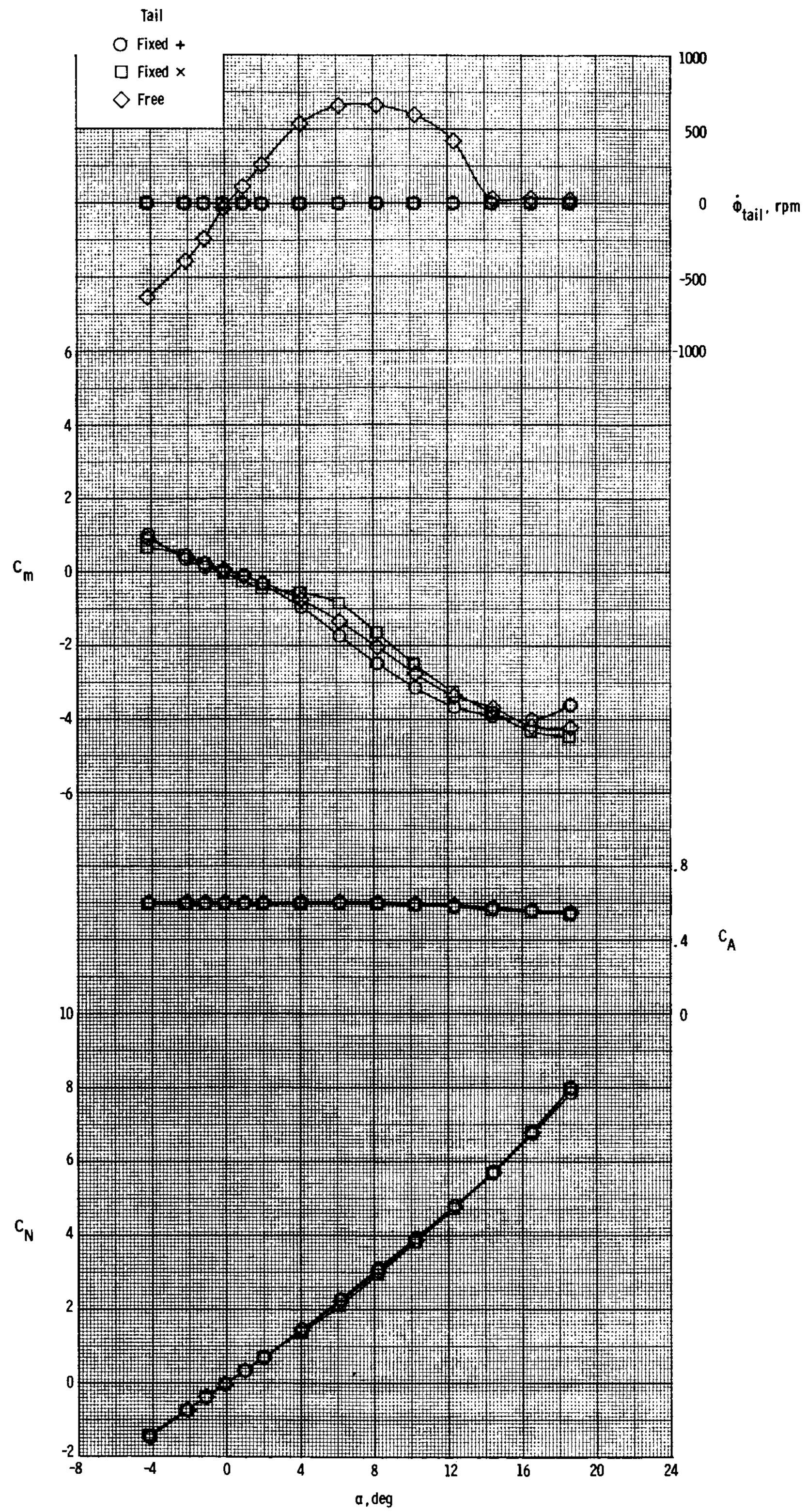


(a) $M = 1.70$.

Figure 6. Effect of fixed and free-rolling tail on longitudinal aerodynamic characteristics of model with canard yaw control. $\delta_{yaw} = -5°$.

ORIGINAL PAGE IS
OF POOR QUALITY

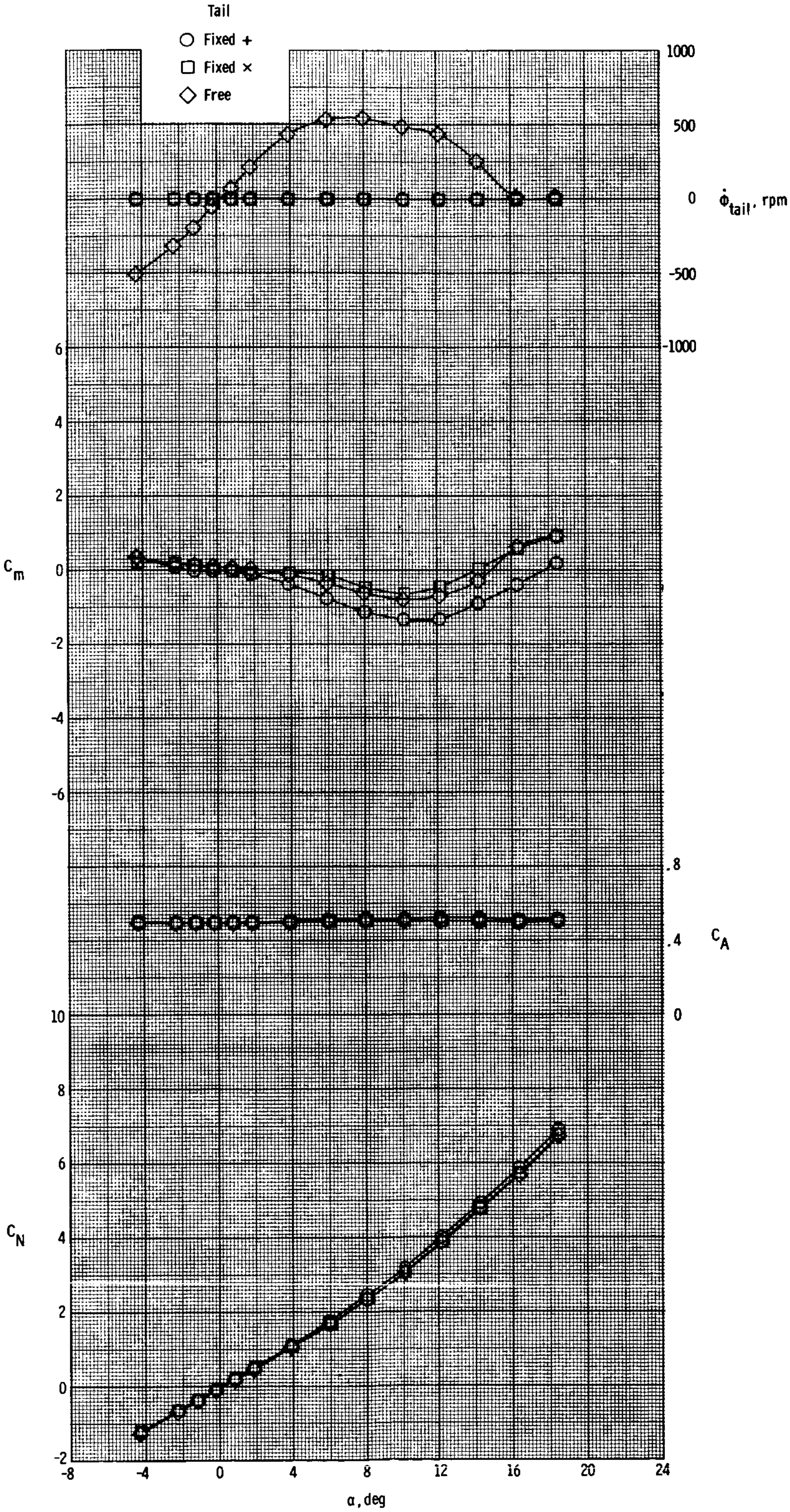


(b) $M = 2.16$.

Figure 6. Continued.

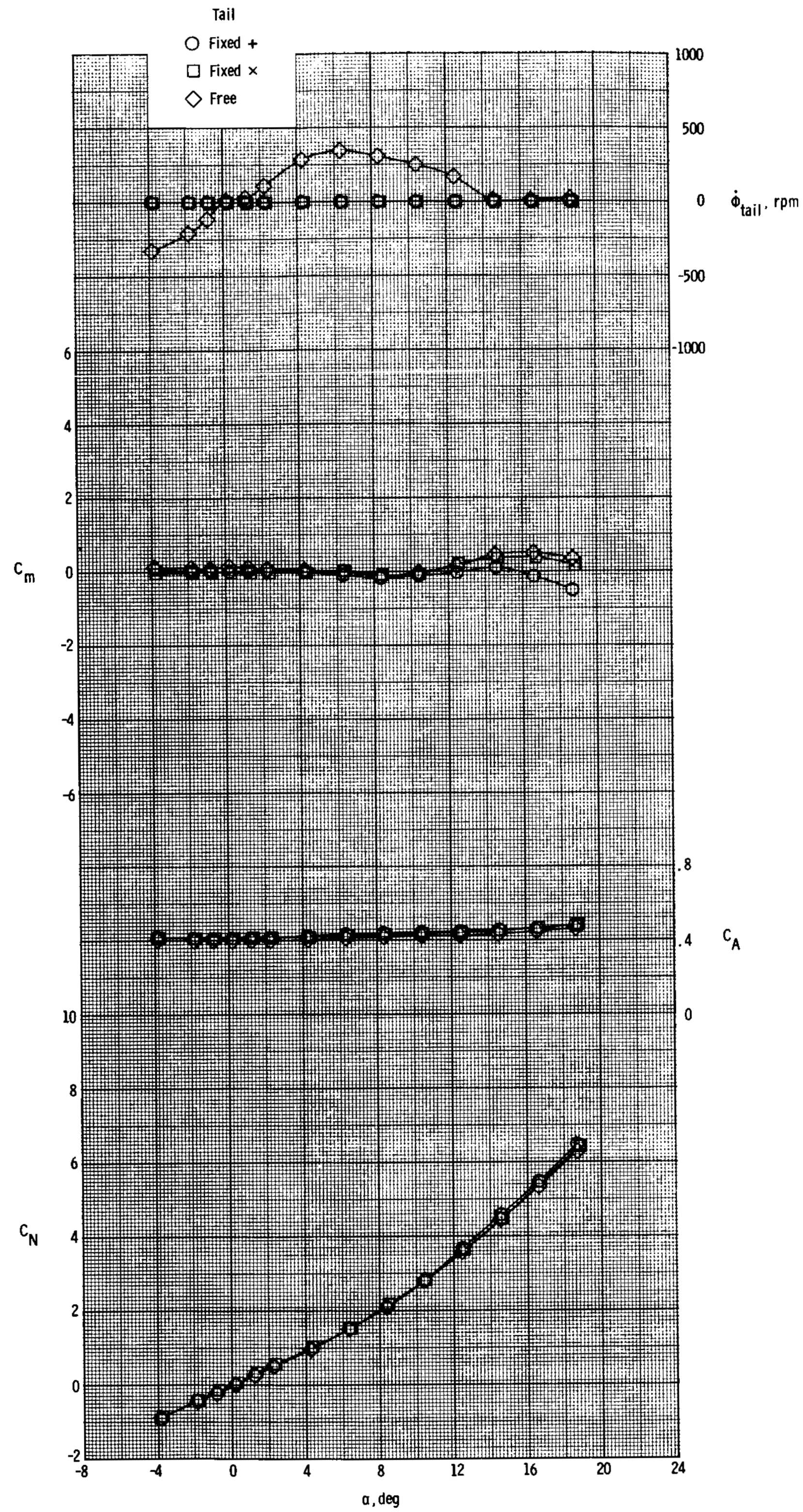


(c) $M = 2.86$.

Figure 6. Concluded.

ORIGINAL PAGE IS
OF POOR QUALITY

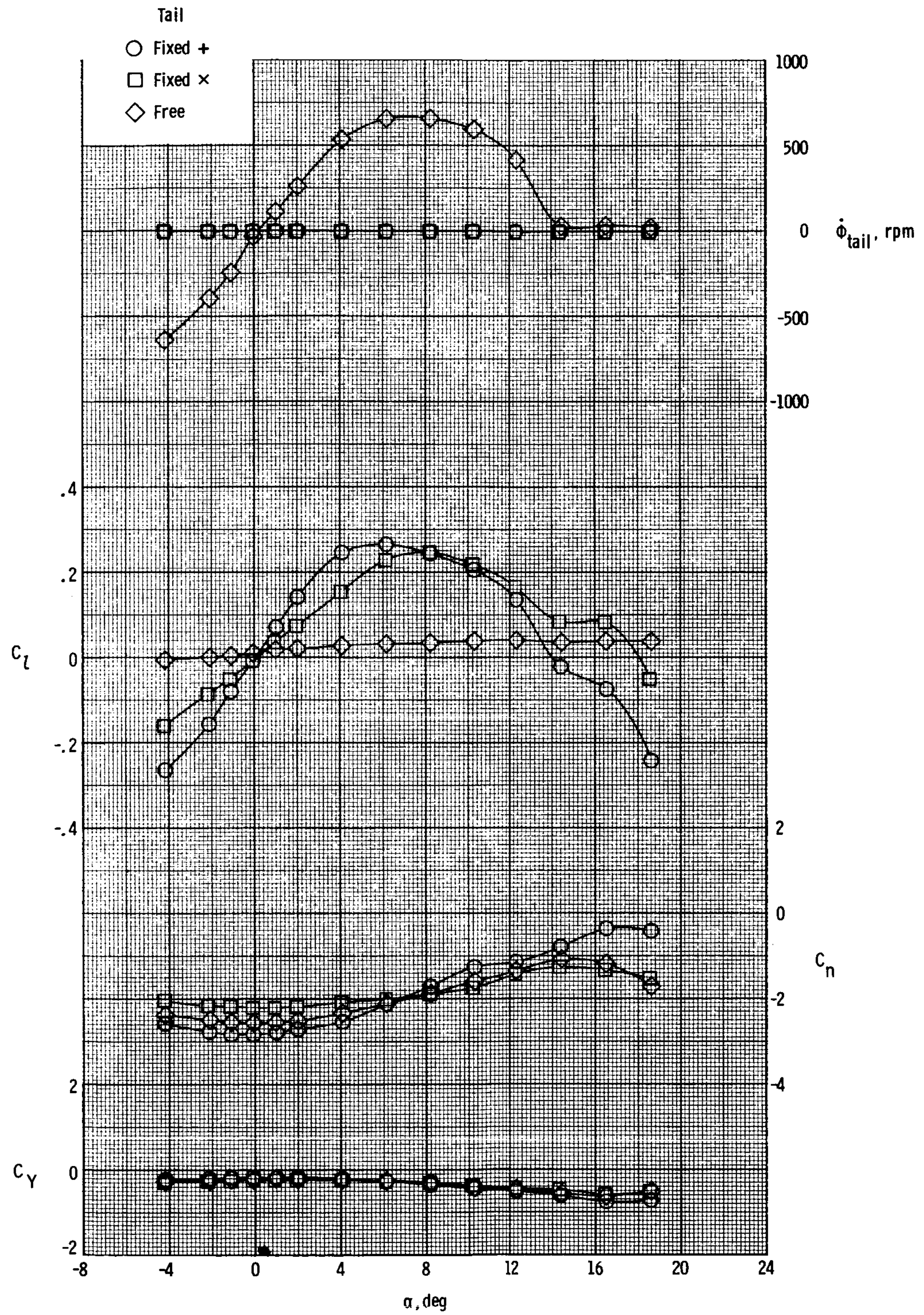


(a) $M = 1.70$.

Figure 7. Effect of fixed and free-rolling tail on lateral-directional aerodynamic characteristics of model with canard yaw control. $\delta_{yaw} = -5°$.

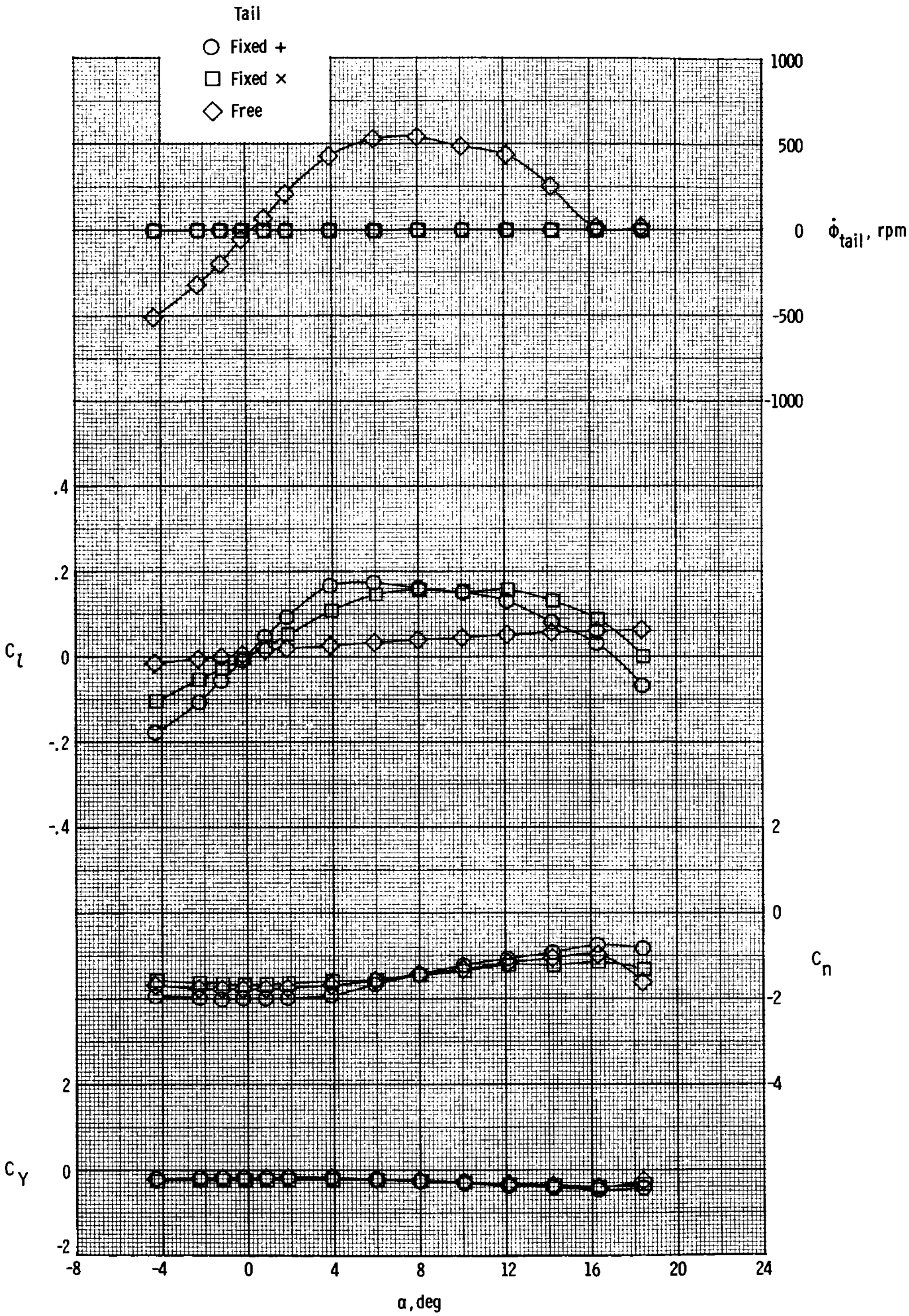


(b) $M = 2.16$.

Figure 7. Continued.

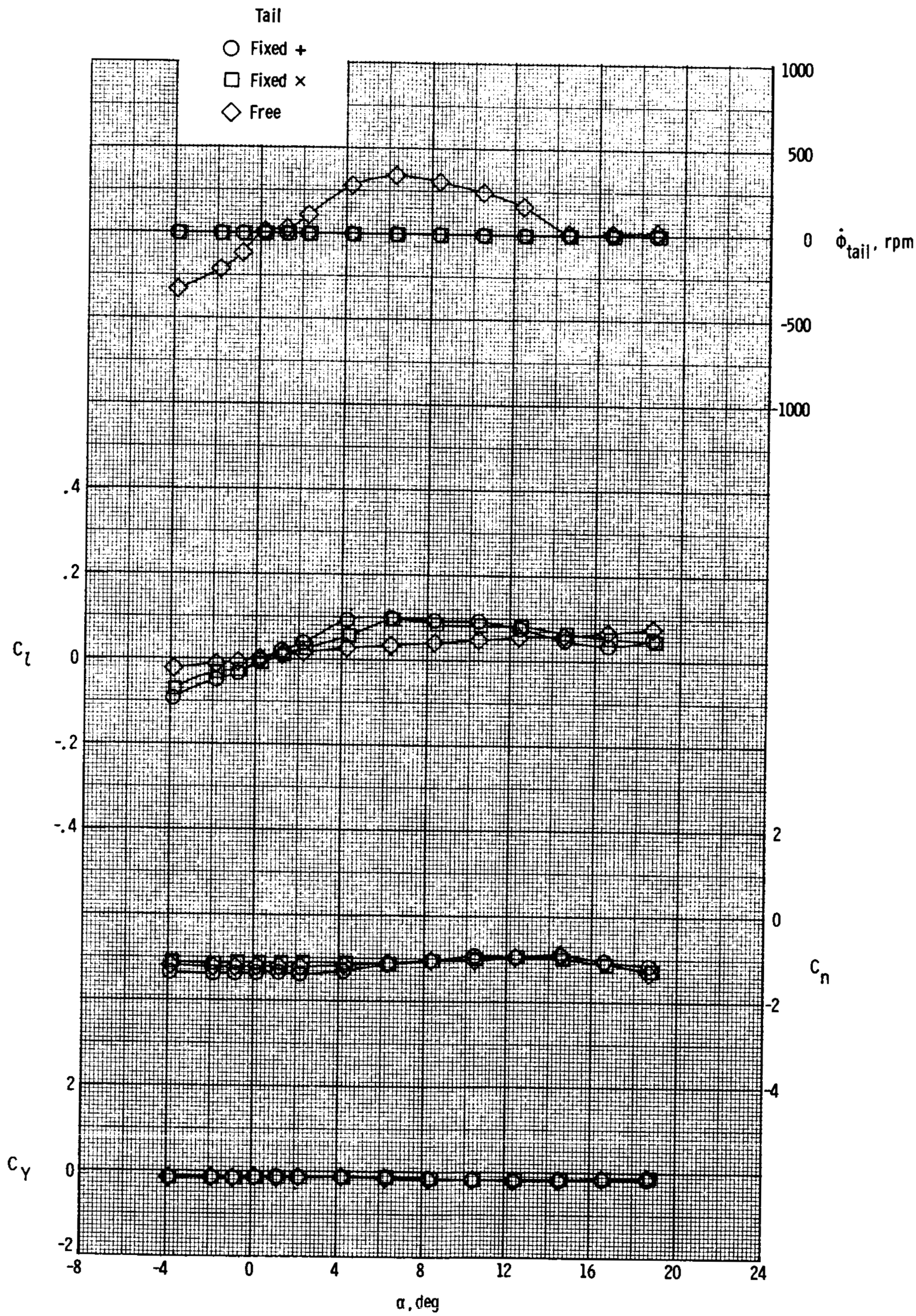


(c) $M = 2.86$.

Figure 7. Concluded.

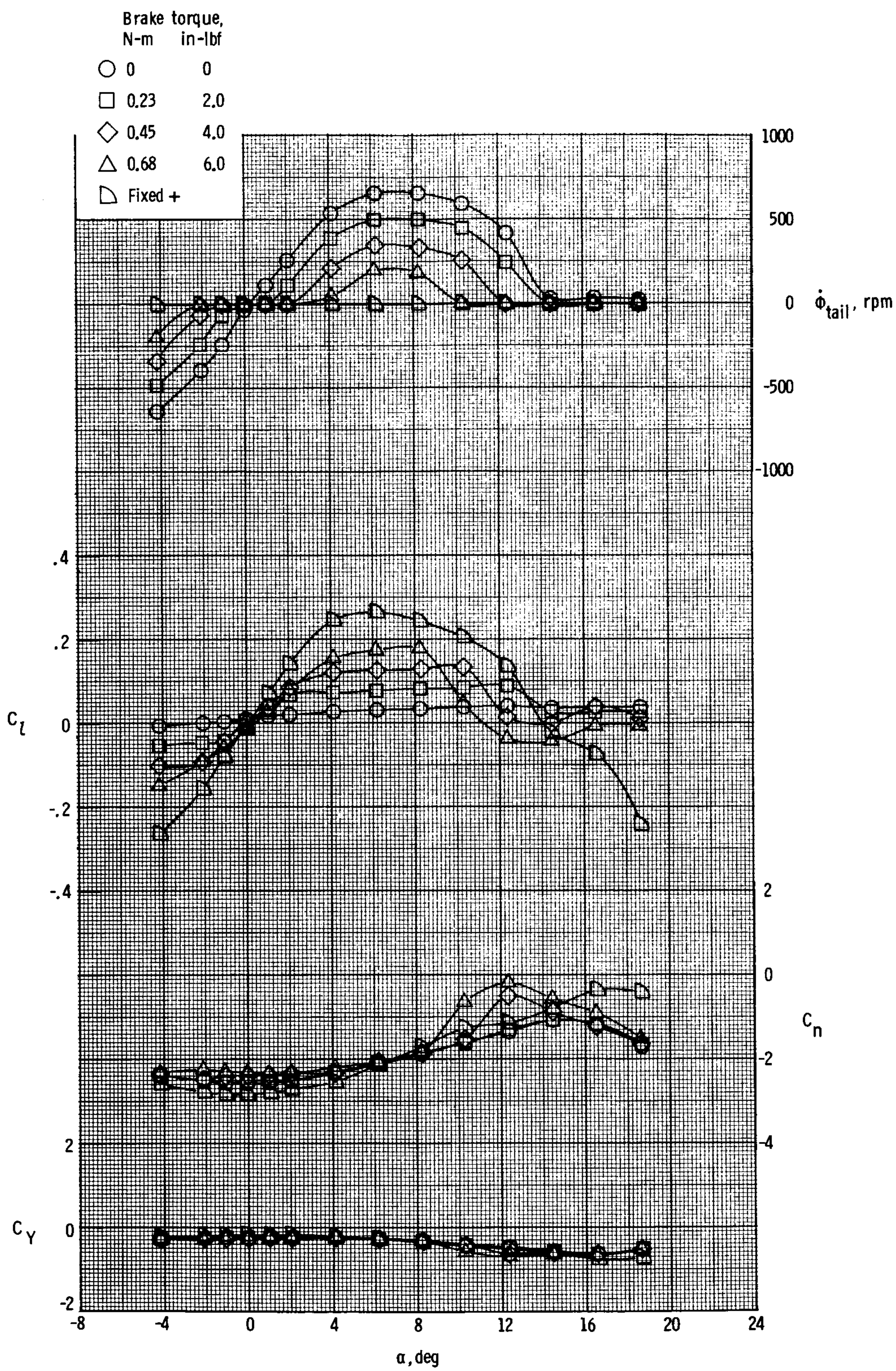


(a) $M = 1.70$.

Figure 8. Effect of command brake torque on lateral-directional aerodynamic characteristics of free-rolling-tail configuration with canard yaw control. $\delta_{yaw} = -5°$.

ORIGINAL PAGE IS
OF POOR QUALITY

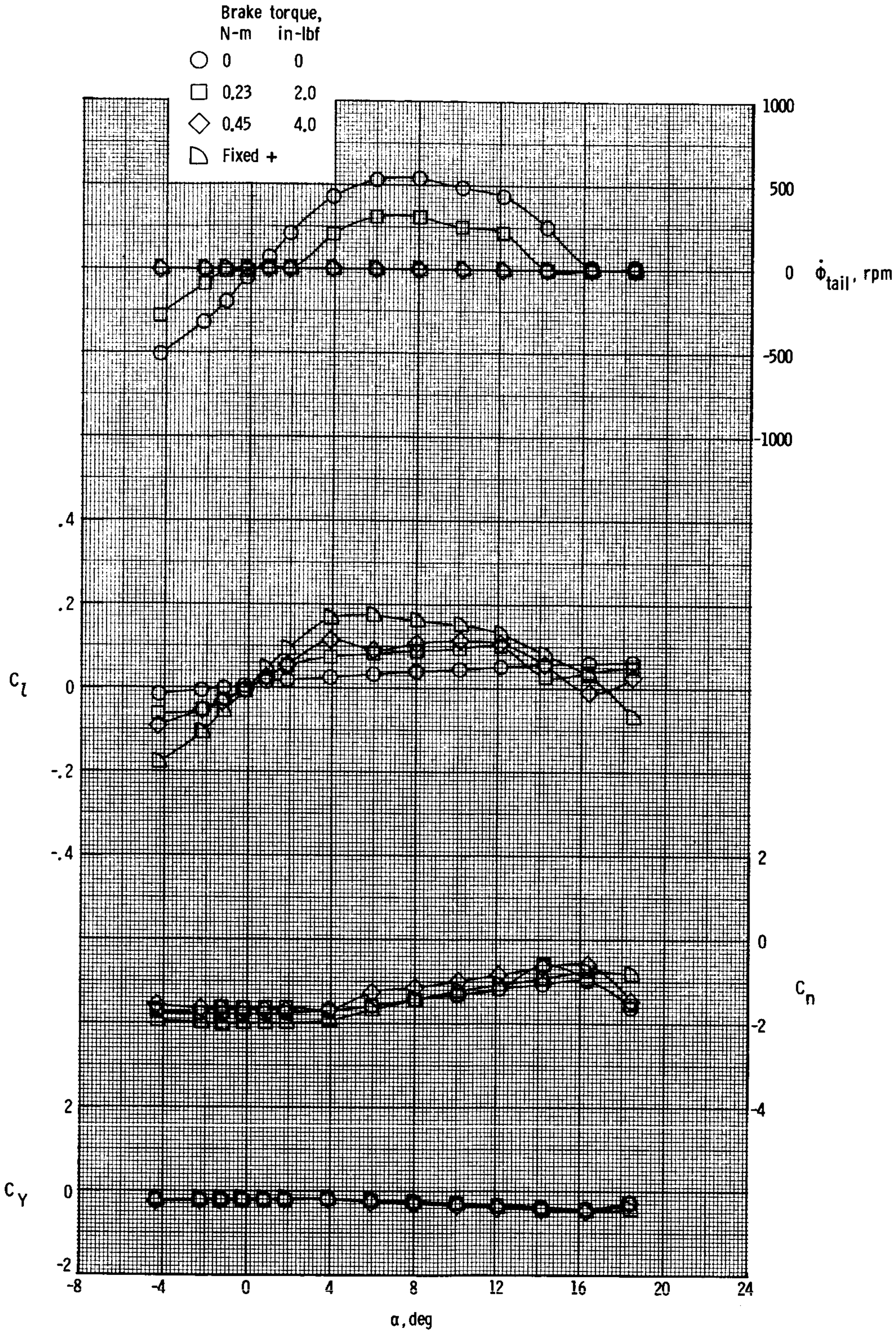


(b) $M = 2.16$.

Figure 8. Continued.

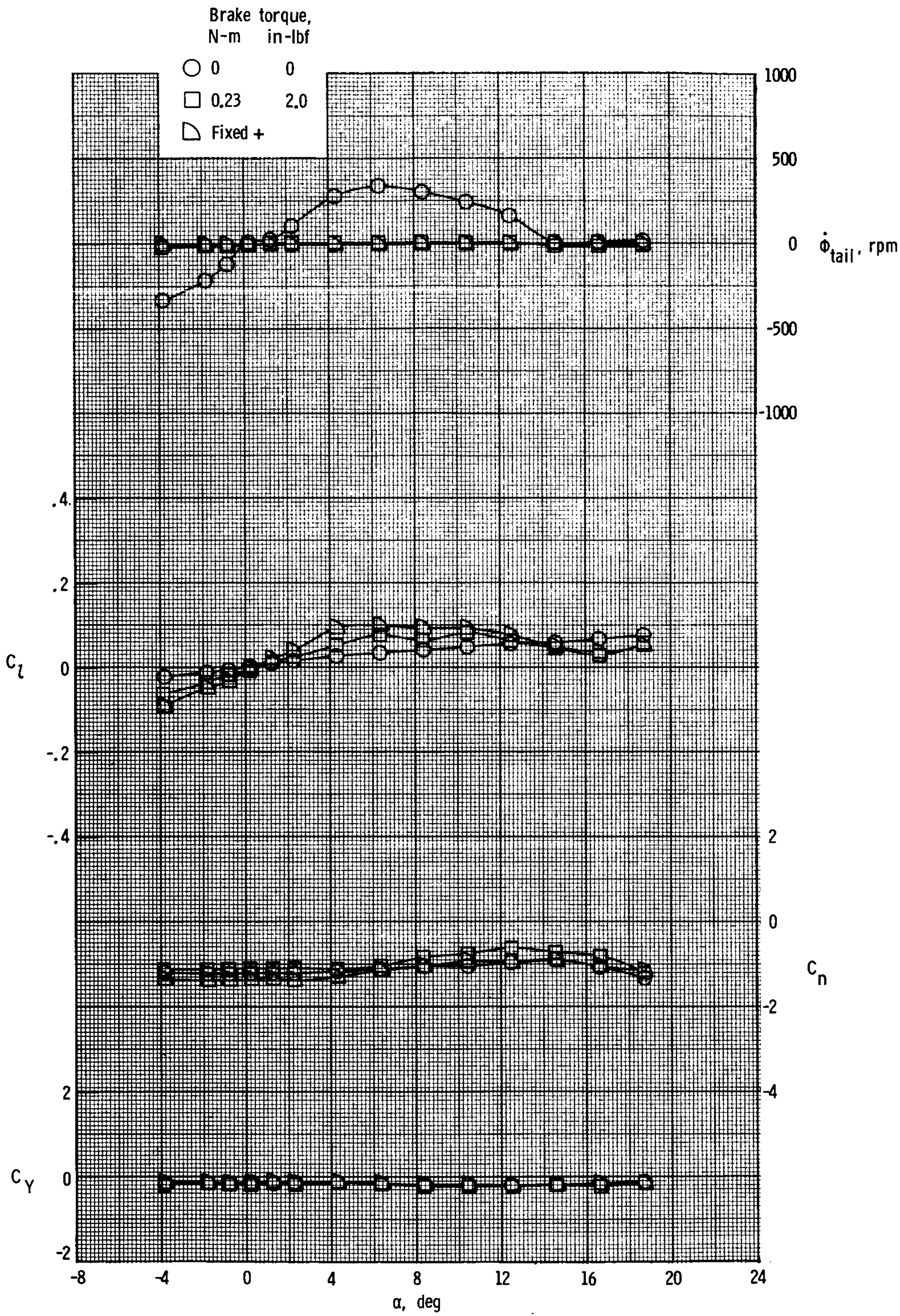


(c) $M = 2.86$.

Figure 8. Concluded.

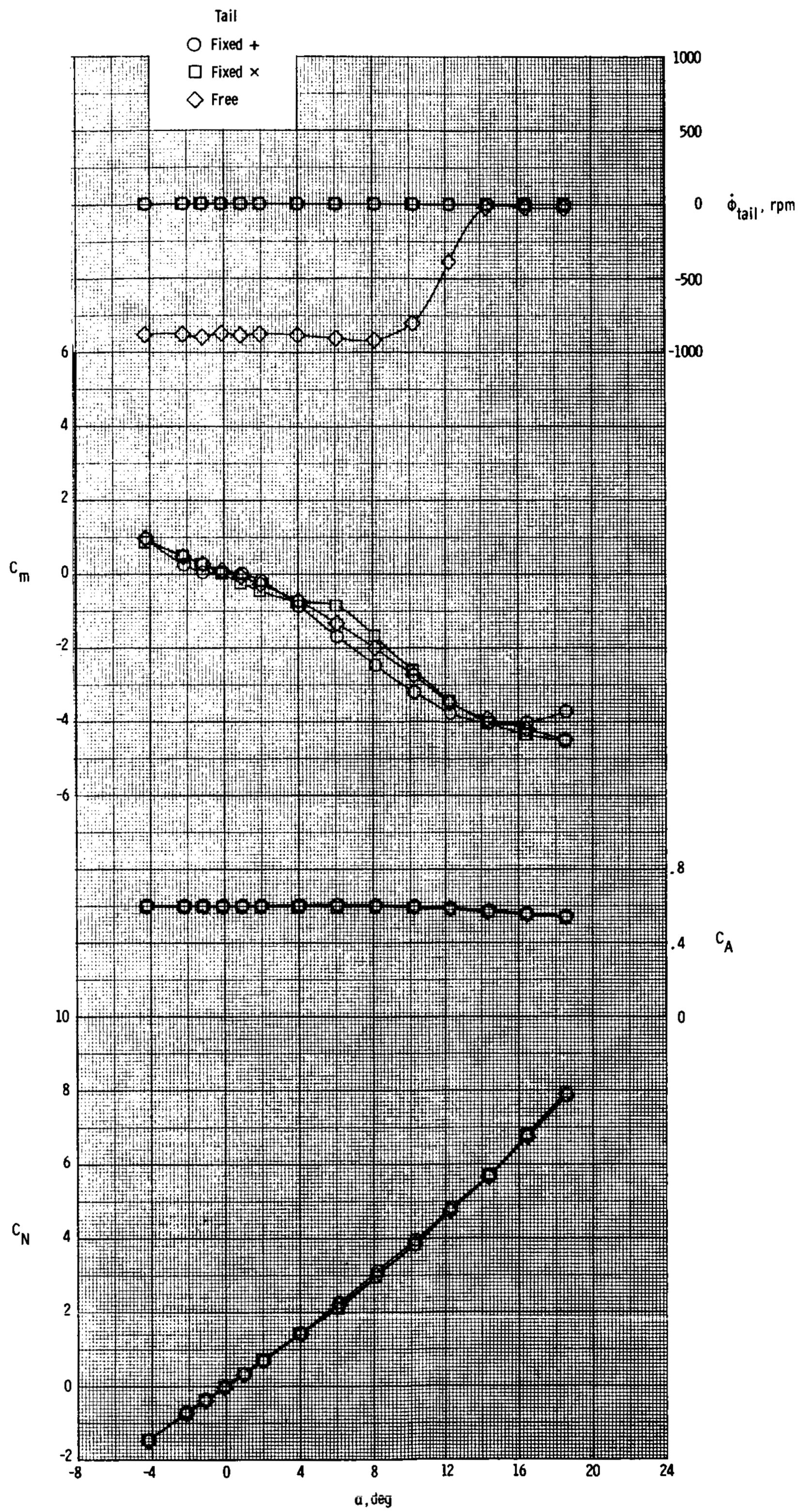


(a) $M = 1.70$.

Figure 9. Effect of fixed and free-rolling tail on longitudinal aerodynamic characteristics of model with canard roll control. $\delta_{roll} = 5°$.

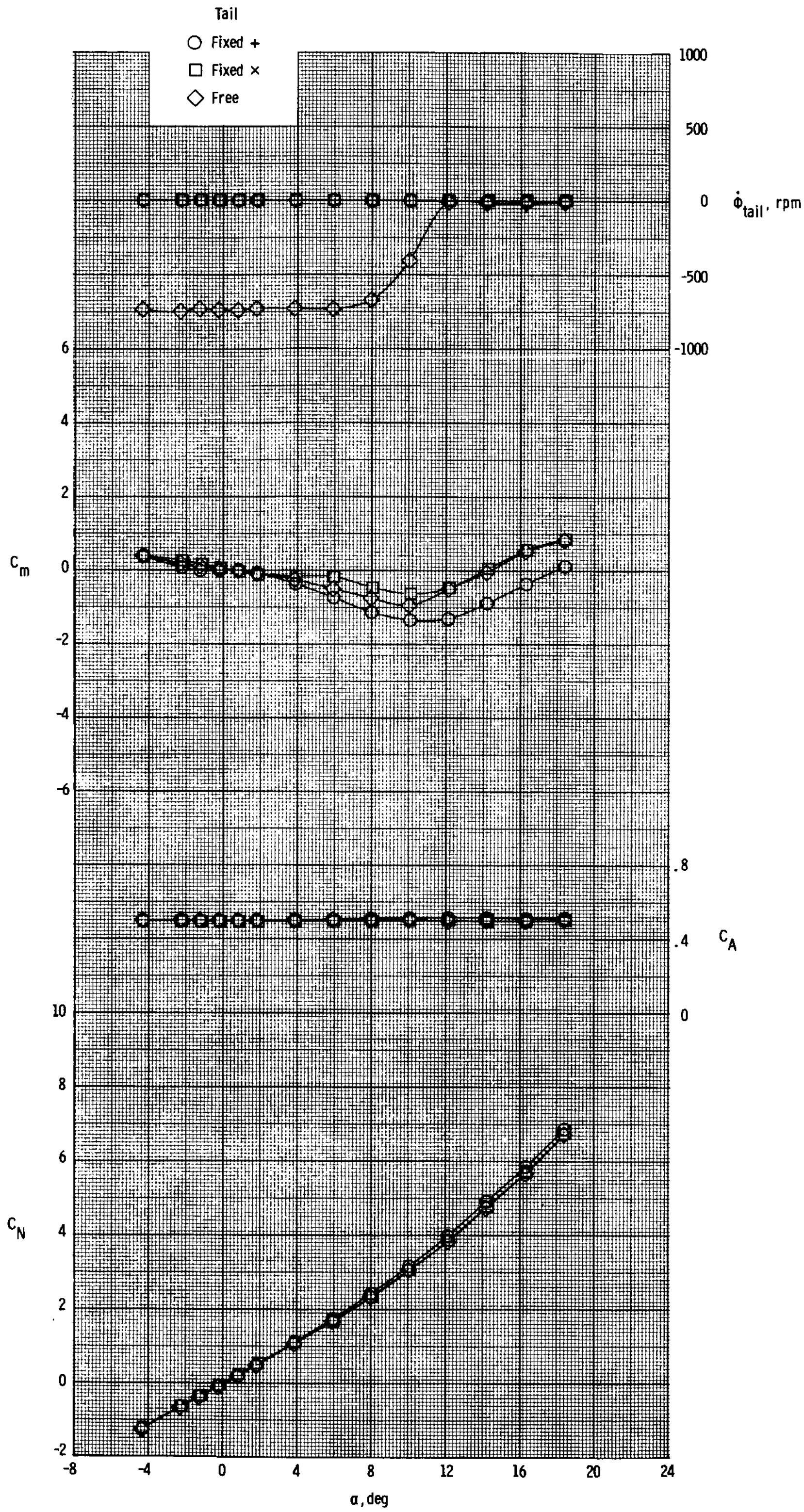


(b) $M = 2.16$.

Figure 9. Continued.

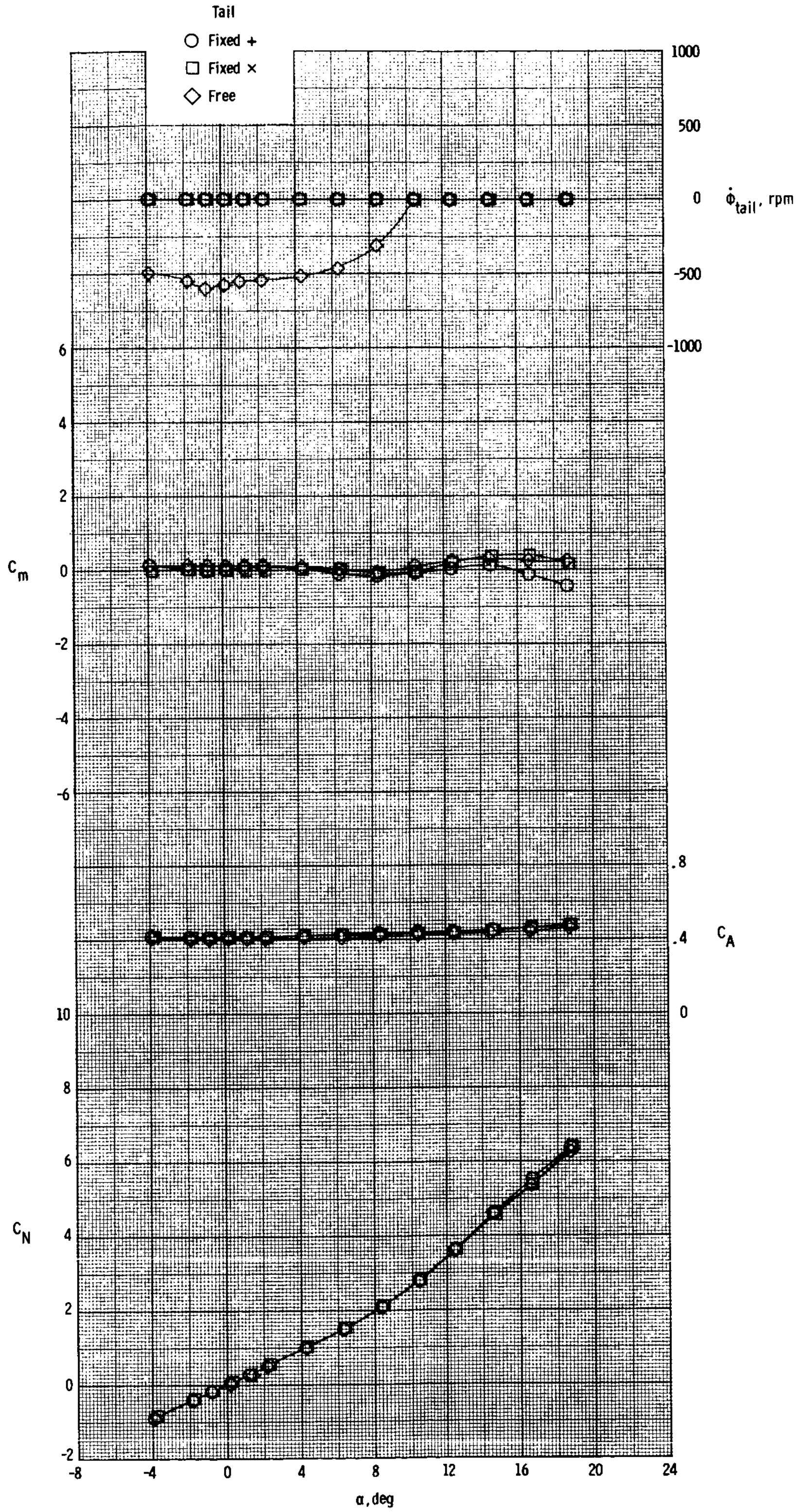


ORIGINAL PAGE IS
OF POOR QUALITY

(c) $M = 2.86$.

Figure 9. Concluded.

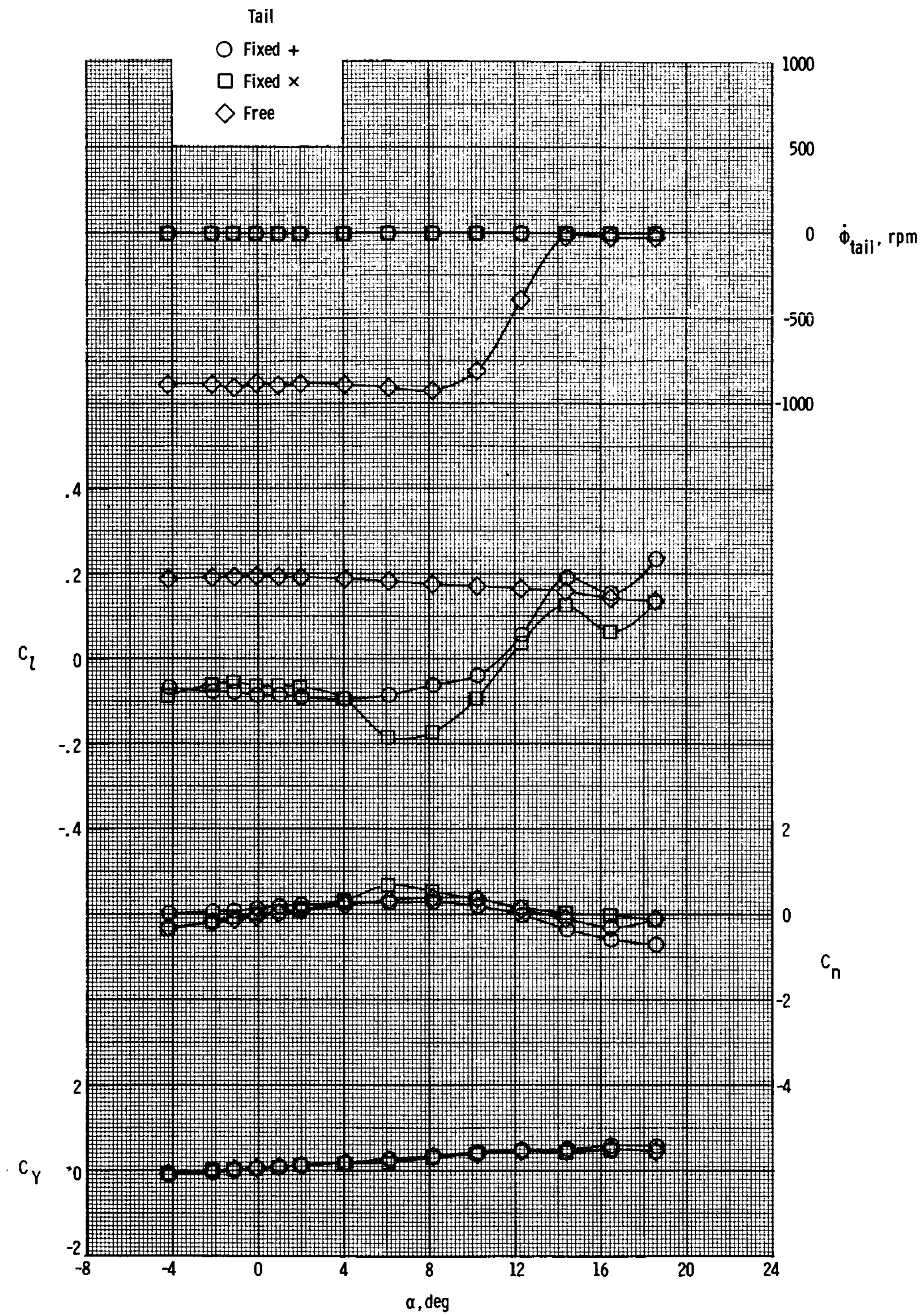


(a) $M = 1.70$.

Figure 10. Effect of fixed and free-rolling tail on lateral-directional aerodynamic characteristics of model with canard roll control. $\delta_{roll} = 5°$.

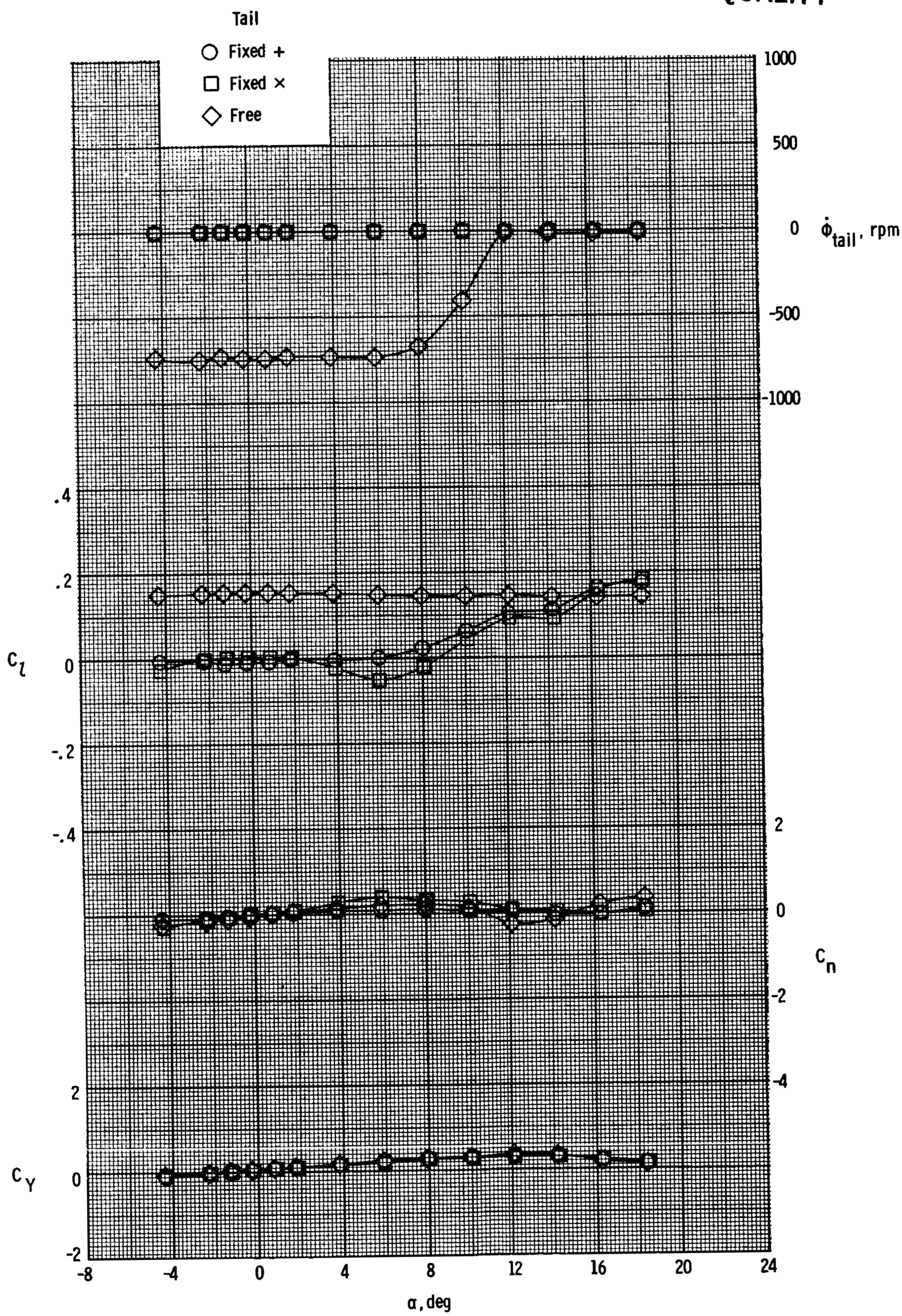


(b) $M = 2.16$.

Figure 10. Continued.

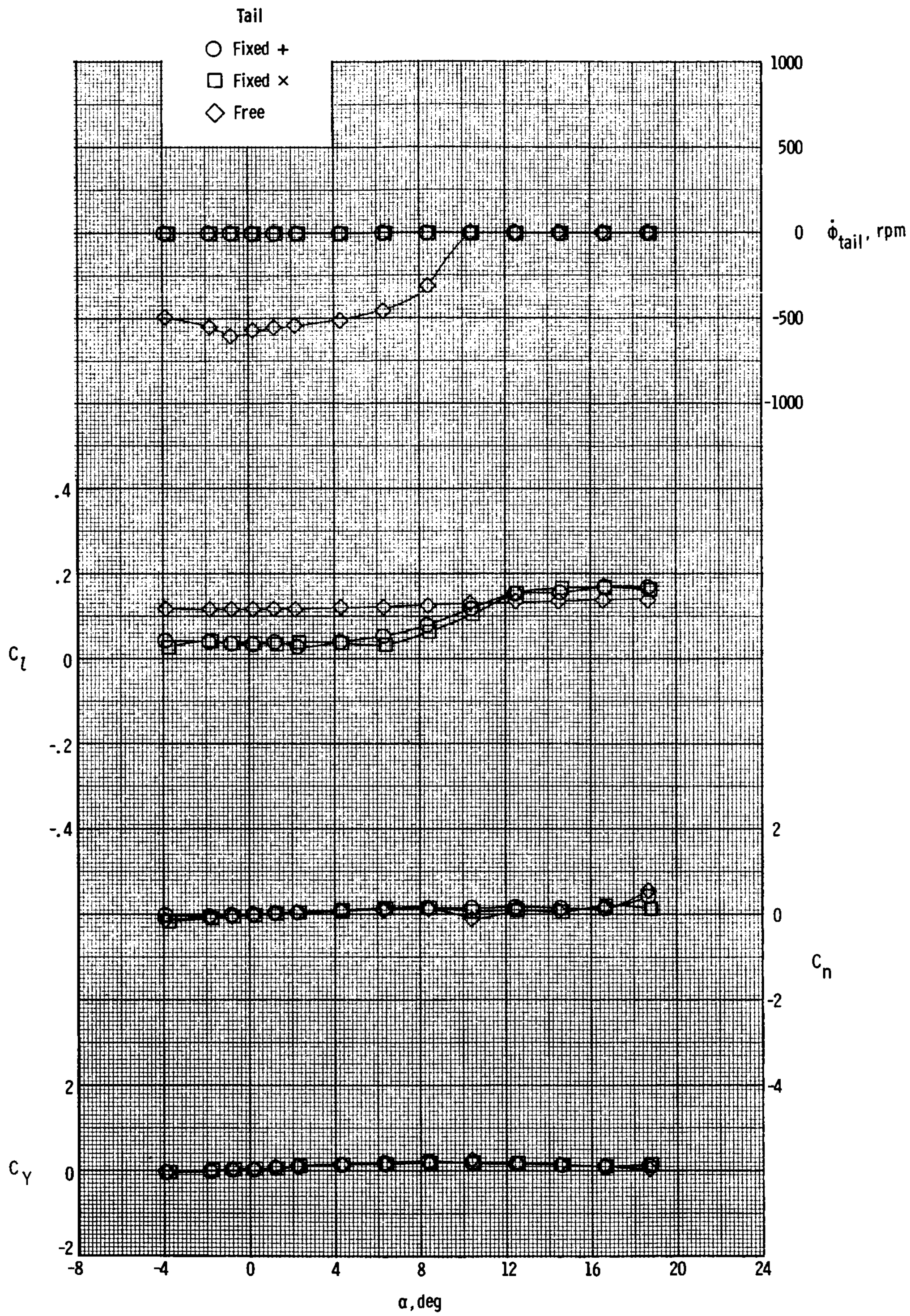


(c) $M = 2.86$.

Figure 10. Concluded.

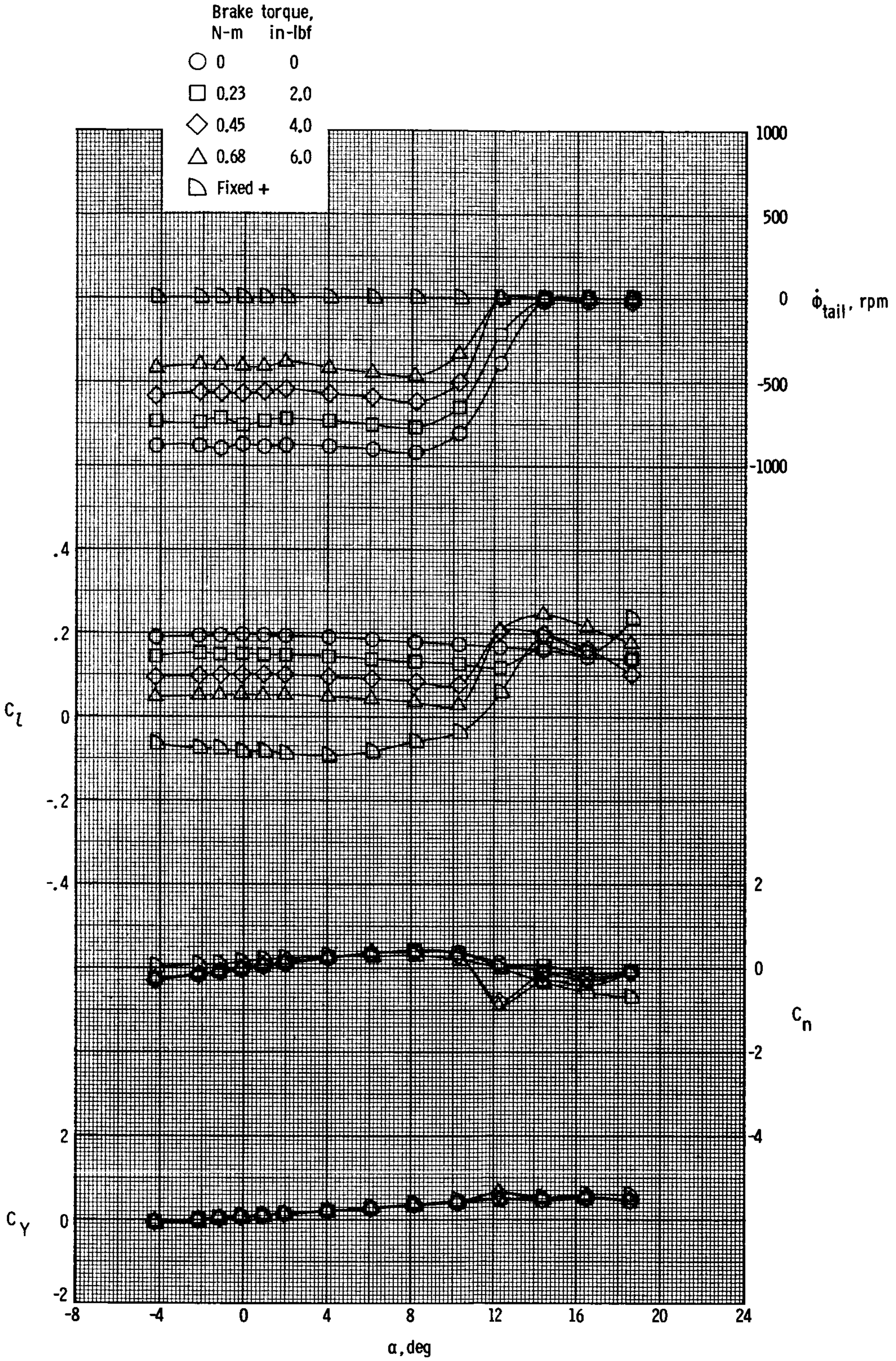


(a) $M = 1.70$.

Figure 11. Effect of command brake torque on lateral-directional aerodynamic characteristics of free-rolling-tail configuration with canard roll control. $\delta_{roll} = 5°$.

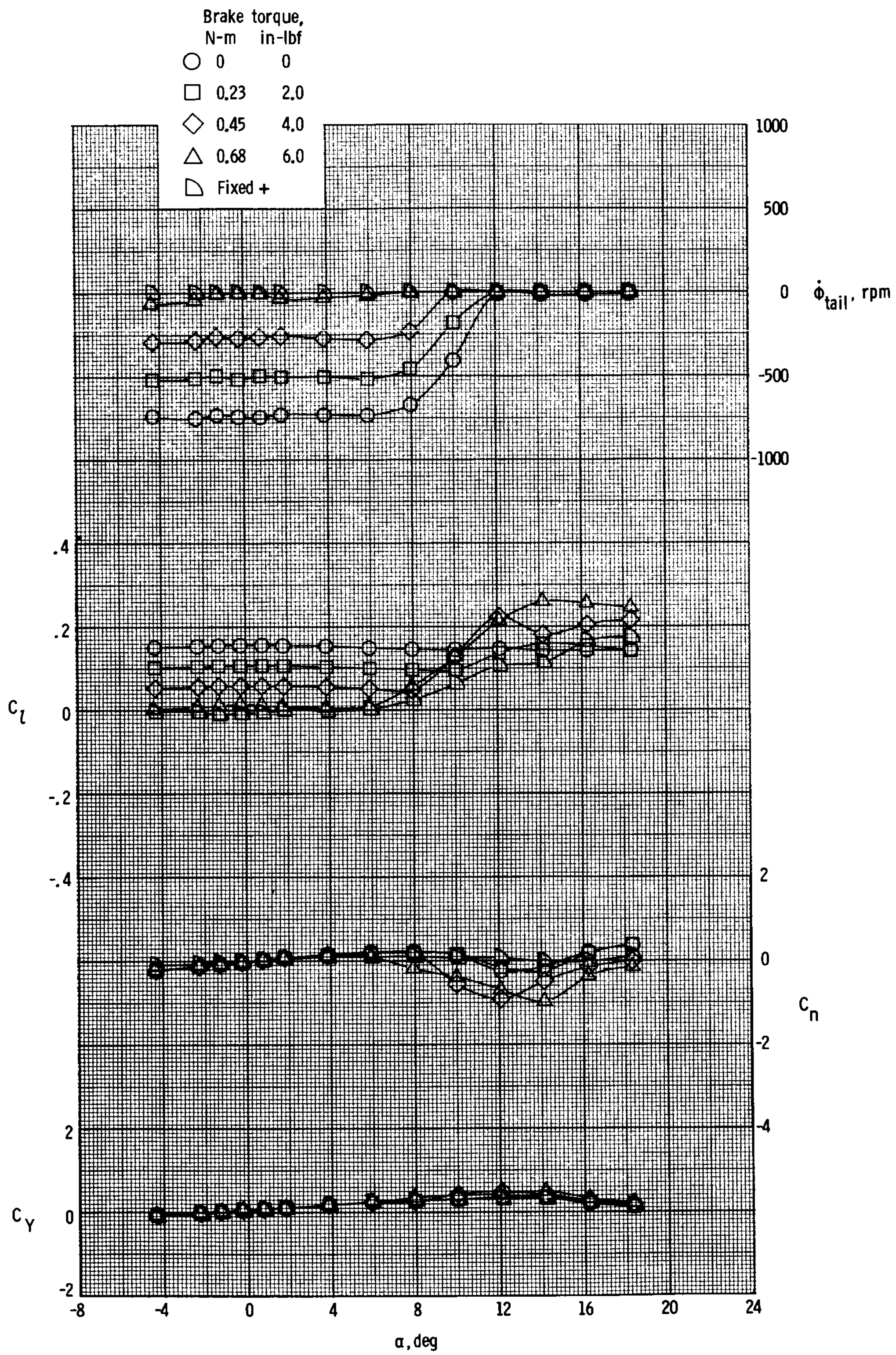


(b) $M = 2.16$.

Figure 11. Continued.

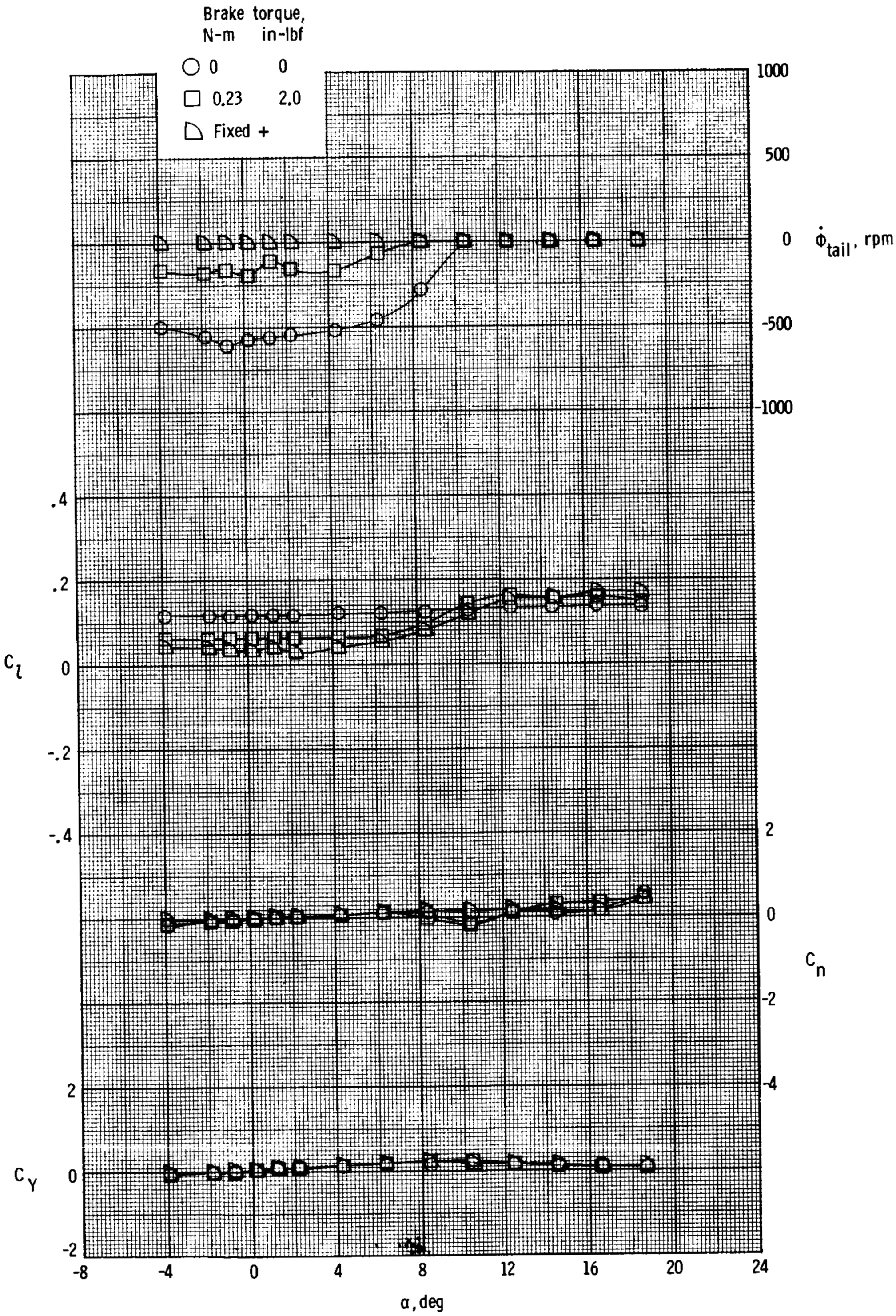


(c) $M = 2.86$.

Figure 11. Concluded.

1. Report No.
NASA TP-2401

2. Government Accession No.

3. Recipient's Catalog No.

4. Title and Subtitle
Wind-Tunnel Investigation at Supersonic Speeds of a Remote-Controlled Canard Missile With a Free-Rolling-Tail Brake Torque System

5. Report Date
March 1985

6. Performing Organization Code
505-43-23-02

7. Author(s)
A. B. Blair, Jr.

8. Performing Organization Report No.
L-15882

9. Performing Organization Name and Address
NASA Langley Research Center
Hampton, VA 23665

10. Work Unit No.

11. Contract or Grant No.

12. Sponsoring Agency Name and Address
National Aeronautics and Space Administration
Washington, DC 20546

13. Type of Report and Period Covered
Technical Paper

14. Sponsoring Agency Code

15. Supplementary Notes

16. Abstract
A wind-tunnel investigation at Mach numbers of 1.70, 2.16, and 2.86 was conducted to determine the static aerodynamic characteristics of a cruciform canard-controlled missile with fixed or free-rolling tail-fin afterbodies. Mechanical coupling effects of the free-rolling-tail afterbody were investigated by using an electronic/electromagnetic brake system that provided arbitrary tail-fin brake torques with continuous measurements of tail-to-mainframe torque and tail roll rate. Remote-controlled canards were deflected to provide pitch, yaw, and roll control. The results of the investigation indicate that the induced rolling-moment coefficients due to canard yaw control are reduced and linearized for the free-rolling-tail (free-tail) configuration. The canards of the free-tail configuration provided conventional roll control for the entire angle-of-attack test range. For the free-tail configuration, the induced rolling-moment coefficient due to canard yaw control increased and the canard roll control decreased with increases in brake torque, which simulated bearing friction torque. It appears that a compromise in regard to bearing friction, for example, low-cost bearings with some friction, may allow satisfactory free-tail aerodynamic characteristics that include reductions in adverse rolling-moment coefficients and lower tail roll rates.

17. Key Words (Suggested by Authors(s))
Supersonic aerodynamics
Missile aerodynamics
Canard-controlled missiles
Free-rolling tail

18. Distribution Statement
[redacted]
Until March 1987

Subject Category 02

19. Security Classif.(of this report)
Unclassified

20. Security Classif.(of this page)
Unclassified

21. No. of Pages
36

22. Price